Late Pliocene Ice Sheets as an Analogue for Future Climate: A Sensitivity Study of the Polar Southern Hemisphere

Katherine Power[1], Fernanda DI Alzira Oliveira Matos[2], and Qiong Zhang[1]

[1]Department of Physical Geography and Bolin Centre for Climate Research, Stockholm University, Stockholm, Sweden
[2]Alfred Wegener Institute - Helmholtz Centre for Polar and Marine Research, Bremerhaven, 27570, Germany

Correspondence: Katherine Power (katherine.power@natgeo.su.se)

Abstract.

The ~~Antarctic and Greenland Ice Sheets (AISand GrIS)~~Earth's ice sheets, including the Antarctic Ice Sheet (AIS), are critical tipping points in the ~~Earth's~~ climate system. ~~Their potential collapse could trigger~~ In recent years, the potential future collapse has garnered increased attention due to its cascading effects, that could significantly alter global climate patterns, and cause large-scale, long-lasting, and potentially irreversible changes within human timescales. This study investigates the large-scale response of the polar Southern Hemisphere (pSH; comprising the Southern Ocean and Antarctica (60-90~~°~~°S)) to the ~~isolated change in albedo resulting from reducing AIS and GrIS to prescribed~~ geometric reduction of ice-sheets to a reconstructed Late Pliocene (LP) extent~~. Using well-documented paleogeography of the LP from the~~ , and imposing increased greenhouse gas forcing in the Earth System. Using the PRISM4D reconstruction, where ice sheets such as the West Antarctic Ice Sheet (WAIS) ~~and the northwestern GrIS~~ were significantly diminished, we conducted ~~multicentennial~~ multi-centennial simulations with the EC-Earth3 model at atmospheric CO_2 concentrations of 280 ppmv and 400 ppmv.

~~Our results reveal that~~ The simulation performed with LP ice sheet extent leads to a 9.5°C rise in surface air temperature, approximately 16% reduction in sea ice concentration over Antarctica and the Southern Ocean. These changes far exceed those driven by CO_2 increase alone, which result in a 2.5°C warming and a 9.3% sea ice decline. ~~Under only CO_2,~~ Additionally, both experiments induce there is a ~~shift towards a more positive~~ reversal in sea level pressure (SLP) polarity with respect to pre-industrial patterns. Higher than normal SLP is present over Antarctica and lower than normal SLP in the mid-latitudes, indicative of a negative phase of the Southern Annular Mode (SAM)~~,~~ . This is supported by a ~~strengthening~~ weakening of the westerly jet ~~. However,~~ which in turn contributes to the formation of a fresh cap in the upper ocean, induced by the imposed climatic impacts of our sensitivity experiments. This overall freshening of the upper ocean increases stratification in the water column and prevents deep convection in the Southern Ocean, and thus the formation of the Antarctic Bottom Water, which is paramount for the ventilation of the global ocean. Overall, our findings suggest that by increasing the atmospheric concentration of CO_2~~increase together with change in~~ , the AABW is suppressed at a multi-centennial timescale, but by reducing the ice sheet extent~~results in a highly varied SAM, a result of a weakening and less stable westerly jet. The combined effects of ice sheet reduction and CO_2 forcing initially reduce Antarctic Bottom Water formation, with major implications for the transport~~ , compensatory mechanisms, involving an extensive salinisation of the ocean interior, trigger partial recovery of this water mass. This emphasizes the non-linearity of the climate system, since consequences of reducing the ice sheets induce an amplified

warming and freshening in the near-surface, whereas it induces opposing mechanisms in the deep ocean that significantly alter the dynamics of water masses ~~associated with the Global Meridional Overturning Circulation due to stronger water column stratification driven by surface freshening and subsurface warming.~~

that feed the AABW. By isolating the ~~direct albedo effect of reducing GrIS and AIS extents,~~ climatic response to ice sheet extent reduction, whilst holding other parameters fixed, this study offers critical insights into the mechanisms driving atmospheric and oceanic variability around Antarctica and their broader implications for global climate dynamics. ~~Although the complete Late Pliocene boundary conditions may serve as a valuable analogue for current and future climate change, excluding the orographic changes allows us to specifically assess the primary role of surface reflectivity. This targeted approachlays the groundwork for future research to explore how the combined effects of albedo and paleogeographical changes could influence interhemispheric climate feedbacks under scenarios of future ice sheet collapse or instability~~Here we provide a unique, targeted approach, specifically focusing on the direct impact of ice sheet retreat on regional climate.

1 Introduction

The ~~Greenland and Antarctic ice sheets(GrIS and~~ Earths ice sheets, including the Antarctic Ice Sheet (AIS hereafter), are pivotal components of the ~~Earth's~~ climate system. Their high albedo reflects a significant portion of solar radiation, thereby cooling surrounding regions and playing a critical role in regulating global air and sea surface temperatures. In addition, these ice sheets influence atmospheric and ~~ocean~~ oceanic circulation at various scales, modulating rates of sea ice and deep water formation as well as the wind regime across different oceanic basins (Clark et al., 1999). However, the stability of these ice sheets is currently at risk due to ~~enhanced melting of their ice, reduction in snowfall,~~ climate change driven enhanced surface and basal melting~~of ice cavities that happen due to climate change and are projecting to~~ , with melting rates projected to intensify in the following decades (Pollard et al., 2015; Song et al., 2025).

Projections indicate that ~~the accelerated loss of the GrIS and AIS~~ accelerated ice sheet loss will have far-reaching implications for global climate dynamics (Naughten et al., 2023; Greene et al., 2024; Buizert et al., 2018). These changes are likely to disrupt critical processes such as deep-water formation and the contribution of the Southern Ocean to global heat transport and carbon sequestration (Cai et al., 2013; Menviel et al., 2023). Understanding these risks is critical, as ~~the potential collapse of the AIS and GrIS~~ potential ice sheet collapse could trigger cascading climate feedbacks, leading to irreversible and long-lasting changes within human timescales.

Paleoclimate records offer unique insights into the behavior of these ice sheets during past warm periods, such as ~~Marine Isotope Stage 5e (~~the Last Interglacial (LIG; ~~125,000 years ago)~~127 kiloyears (ka)) in the Pleistocene (Steig et al., 2015) and the Late Pliocene Age (LP; ~3,3 million years ago) (Naish et al., 2009; Kim and Crowley, 2000)~~. These periods were characterised by significantly smaller ice sheets~~ , when the ice sheets were significantly smaller than today. Using these periods as analogs, we can better understand how ice sheet dynamics influence oceanic and atmospheric processes in climates warmer than today, which can offer valuable lessons for predicting future climate behavior as the Earth continues to warm.

~~Paleoclimate~~ However, as the LIG entails orbit-induced changes in insolation with respect to the modern climate (Otto-Bliesner et al., 201
, paleoclimate insights from the Late Pliocene are increasingly used as analogues for future warm climate states, offering critical context for how Earth's climate system may respond to elevated CO_2 ~~levels. Studies focusing on the Greenland Ice Sheet have demonstrated the importance of surface albedo feedbacks when considering future climate change, based on LP evidence (Power et al., 2023). de Nooijer et al. (2020) investigation of Arctic conditions during the LP gives insight to future conditions, as does Feng et al. (2017) work identifying amplified LP Arctic warming through~~ $_2$ levels, while at similar orbital configuration. The period was characterised by atmospheric CO_2 concentrations broadly comparable to present-day values, estimated at 350–450 ppmv (Haywood et al., 2016b). Global mean surface temperatures were 2-4°C higher than pre-industrial, with amplified warming at high latitudes. In the Southern Hemisphere, evidence suggests substantially reduced AIS extent, particularly the WAIS, and the retreat of marine-based sectors in East Antarctica (Dolan et al., 2018). Southern Ocean sea ice was likely seasonally absent or greatly reduced, accompanied by displaced westerly winds and changes in Antarctic Bottom Water (AABW) formation, with implications for Antarctic climate feedbacks and ice-ocean interactions. The combination of near-modern greenhouse gas concentrations, polar amplification, reduced AIS extent and reorganised Southern Ocean circulation makes the Late Pliocene a valuable paleo-analogue for projected future change. Polar amplification ratios for the period have been estimated at around 2.3 (de Nooijer et al., 2020), closely aligning with future projections ranging between 2.11 and 2.76 depending on the chosen scenario (Xie et al., 2022; Pörtner et al., 2022). Both Chandan and Peltier (2018) and Lord et al. (2017) demonstrate how bridging LP knowledge and future projections improve our understanding on how sensitive the Earth's climate is to various forcings. Simulating the climate of the Late Pliocene is a core component of the Pliocene Model Intercomparison Project (PlioMIP) Haywood et al. (2016a, 2022), which facilitates international multi-climate model comparisons for the Pliocene epoch Haywood et al. (2010). Contributions from PlioMIP have been integral to the Intergovernmental Panel on Climate Change (IPCC) 5th Stocker et al. (2013) and 6th Assessment Reports gul (2022). By providing insight into analogous climate forcings, the Late Pliocene offers a unique framework for understanding the long-term stability of the AIS and its impact on the Southern Ocean dynamics in a warming world.

However, existing work on the LP as a warm climate analogue heavily focuses on Arctic processes, demonstrating the significance of surface albedo feedbacks involving the Greenland Ice Sheet (GrIS) retreat when considering future climate change (Power et al., 2023), identifying which key oceanic gateways ~~, and Lunt et al. (2012) understanding of~~ amplified LP Arctic warming (Feng et al., 2017) and may do so again. Additionally, by understanding Pliocene polar amplification ~~has aided our knowledge of~~ (Lunt et al., 2012; de Nooijer et al., 2020), more accurate projections can be made for amplification in a prospective warming world. ~~Both Chandan and Peltier (2018) and Lord et al. (2017) demonstrate how bridging LP knowledge and future projections improve our understanding.~~ In the Southern Hemisphere, the role of the ~~Antarctic Ice Sheet~~ AIS in modulating future climate is gaining attention ~~. Weiffenbach et al. (2024) show that mid-Pliocene simulations with a reduced AIS result in substantial Southern Ocean warming. This is primarily driven by sea ice loss, leading to stronger surface stratificationand a weakening of the deep abyssal overturning circulation. Such changes in ocean structure and circulation provide valuable lessons for interpreting future AIS retreat under global warming. Building on these studies, our work offers a unique contribution by isolating the impact of surface reflectivity changes associated solely with GrIS and AIS reduction,~~

~~independently of topographic or vegetation feedbacks, and without freshwater inputs. This allows us to better understand how albedo feedbacks influence ocean-atmosphere interactions in the Southern Hemisphere in a warmer world.~~ (Weiffenbach et al., 2024) , although significant uncertainties remain in understanding the Southern Hemisphere response to changing ice sheets, including mechanisms driving Southern Ocean stratification, AABW formation and coupled atmosphere-ocean feedbacks specific to Antarctica.

Addressing these gaps is critical for constraining the sensitivity of the Antarctic climate system to sustained elevated greenhouse gas forcing. In this study, we replace the modern ice sheet mask of the EC-EARTH3 model with that of the Late Pliocene reconstruction provided by the Pliocene Model Intercomparison Project, phase 3 (PlioMIP3; (Haywood et al., 2024)). We ~~do not modify, however,~~ perform three sensitivity experiments applying modern and LP ice sheet masks under two CO_2 concentrations (280 ppmv and 400 ppmv), whilst not modifying any other model boundary condition representative of the pre-industrial (PI; 1850 CE) Earth's geography. ~~We perform sensitivity experiments applying these two ice sheet masks and multiple CO_2 concentrations.~~ This approach allows us to assess the sensitivity of the climate system to changes in ice sheet extent and varying CO_2 concentrations, using ice sheet conditions of the past as an analogue for the future. ~~By focusing on the albedo effect and excluding orographic changes , our~~ Our work offers a unique contribution by isolating the impact of surface reflectivity changes associated solely with the reduction of ice sheet extent, independently of topographic or vegetation feedbacks and without freshwater inputs, allowing us to better quantify the role of the AIS in modulating Antarctic climate and Southern Ocean circulation. Our goal is to uncover the key mechanisms and processes that could profoundly influence Earth's future climate, environment and societies.

2 Model configuration and experiments setup

2.1 Model configuration

We use the low-resolution configuration of the EC-Earth model, EC-Earth3-LR, an Earth System Model (ESM) developed collaboratively by the European research consortium EC-Earth. EC-Earth model has flexible configurations that allow for the inclusion or exclusion of various climate processes, making it a versatile tool for a wide range of climate studies (Döscher et al., 2022). EC-Earth3 integrates several key components, including the atmospheric model IFS cycle 36r4, the land surface module HTESSEL, the ocean model NEMO3.6 (Madec, 2008) and the sea-ice module LIM3 (Vancoppenolle et al., 2012), all coupled via the OASIS3-MCT coupler (Craig et al., 2017). IFS and HTESSEL have a horizontal linear resolution of TL159 (~~1.125°~~1.125°), and the ocean and sea-ice components (NEMO and LIM) have a nominal resolution of ~~1°~~ 1° (Döscher et al., 2022).

The low-resolution configuration was selected to significantly reduce computational costs ~~, allowing~~ and because it has been extensively validated in both modern and paleo-climate studies, showing robust performance in simulating the climates of past warm periods such as mid-Holocene, Last Interglacial and Late Pliocene (Zhang et al., 2021; Chen et al., 2022; de Nooijer et al., 2020; Har . These simulations have provided valuable information that has been integrated to major model intercomparison projects, such as PMIP4 (Paleoclimate Model Intercomparison Project phase 4) and PlioMIP2 (Pliocene Model Intercomparison Project

phase 2) (Haywood et al., 2020, 2024). Our setup allows for conducting multi-centennial simulations and various sensitivity experiments. This setup , being is particularly suited for exploring slow processes in the deep ocean, which are central to the goals of this study. Such processes include changes in stratification, overturning circulation, Antarctic Bottom Water and AABW formation in response to altered climate forcing.

Overall, The EC-Earth3 model has consistently demonstrated its effectiveness in capturing key climate dynamics, including temperature variability, heat fluxes and other essential aspects of the Earth's System. This capability facilitates a more comprehensive understanding of the impacts of natural and anthropogenic forcing on the global climate system (Koenigk et al., 2013; Döscher et al., 2022; Cao et al., 2023). EC-Earth3 has been extensively validated in both modern and paleo-climate studies, showing robust performance in simulating the climates of past warm periods such as mid-Holocene, Last Interglacial and Late Pliocene (Zhang et al., 2021; Chen et al., 2022; de Nooijer et al., 2020; Han et al., 2024). These simulations have provided valuable information that has been integrated to major model intercomparison projects, such as PMIP4 (Paleoclimate Model Intercomparison Project phase 4) and PlioMIP2 (Pliocene Model Intercomparison Project phase 2) (Haywood et al., 2020, 2024).

2.2 Experiments setup

To investigate the impacts of varying ice sheet extent and CO_2 CO_2 concentrations in the polar Southern Hemisphere (pSH), we performed a series of sensitivity experiments, displayed in Table 1. These experiments employed modern The experiment design is based on the Core and Tier 2/Extension experiments as outlined in the Pliocene for Future protocol of PlioMIP2 and PlioMIP3 Haywood et al. (2016a, 2022). These experiments also follow PlioMIP2 naming convention in which the experiments with modern modern ice-sheet extent (labeled E) are labeled E, and Late Pliocene ice-sheets (labeled Ei) under two atmospheric CO_2 levels: are labeled Ei, followed by their atmospheric CO_2 levels. In our simulations, the experiment E280, comprises the CO_2 concentration reconstructed for the pre-industrial (period (PI; 280 ppmv)and intermediate (, while the experiments E400 and Ei400 employed the reconstructed CO_2 concentration of the Late Pliocene (LP; 400 ppmv). All simulations were started in parallel after branching off from a quasi-equilibrated PI spinup spanning 800-years, to ensure consistent baseline conditions and that any changes observed in the simulations are due to the perturbation and not model drift. We defined quasi-equilibrium as a global surface air temperature trend of less than 0.05 K per century. Thus, the E280 experiment represents our Pre-Industrial control simulation, which is a core experiment of PlioMIP2/3, while E400 and Ei400 represent our sensitivity experiments, being comprised within the Tier 2 experimental design of PlioMIP2 and continuing as optional but pivotal experiments in PlioMIP3 (Haywood et al., 2020, 2024). Specifically, the primary purpose of the E400 experiment is to clarify how an elevated CO_2 level with respect to PI, without other boundary condition changes, affects climate, a process usually referred to as forcing factorization, that isolate CO_2 driven climate change from other paleoclimate forcings. Conversely, Ei400 focuses on the combined impact of CO_2 and ice sheet extent change. Here we define the polar Southern Hemisphere as our domain of study. That includes the entire Southern Hemisphere from 60°Sto 90°S. 60-90°S. To ensure consistency across all simulations, modern vegetation, as simulated for the year 1850 CE, was held fixed by disabling the off-line LPJ-GUESS dynamic vegetation model (Chen et al., 2021). The final 200 years of model output is used for analysis of the mean state, with the pre-industrial control (E280) simulation serving as a baseline for comparison with the sensitivity experiments.

Table 1. The ~~four~~ Core and Tier 2 Pliocene for Future protocol experiments conducted. PI refers to pre-industrial conditions, LP for Late Pliocene. Name terminology is from (Haywood et al., 2016a)

Experiment ID	Ice sheet extent	LSM	Topography	Vegetation	~~CO_2~~CO_2 (ppm)	Orbit
E280	PI	PI	PI	PI	280	PI
E400	PI	PI	PI	PI	400	PI
~~Ei280 LP PI PI PI 280 PI~~ Ei400	LP	PI	PI	PI	400	PI

The protocol for our pre-industrial (PI) simulation follows Eyring et al. (2016) framework for the Coupled Model Intercomparison Project version 6 (CMIP6) *piControl* experiment. Ice sheets, land geography, topography and vegetation are all unmodified from the model. GHG concentrations for CO_2, CH_4 and N_2O are 284.3 ppmv, 808.2 ppbv, and 273.0 ppbv, respectively. For orbital parameters; eccentricity set at 0.016764, obliquity 23.549 and perihelion - 180 is 100.33.

The aim of these sensitivity experiments is to unveil the isolated impact of ~~abruptly shrinking of the AIS and GrIS~~ LP ice sheet extent to the climate of the polar Southern Hemisphere~~. Therefore, Ei simulations involve changing only ice sheet extent for the Greenland Ice and Antarctic Ice Sheets (Haywood et al., 2016a; Chandan and Peltier, 2018). LP AIS~~ , without introducing confounding factors. To achieve this, we modify only the ice sheet mask to represent LP ice sheet extent while retaining pre-industrial albedo values and topography in the model. The LP AIS reconstruction was originally developed using the high-resolution British Antarctic Survey Ice Sheet Model, integrated with climatologies from the Hadley Centre Global Climate Model (Hill et al., 2007; Hill, 2009), utilising PRISM2 boundary conditions (Dowsett et al., 1999). The reliability of the AIS extent is further supported by the results of the PLISMIP results, which evaluated the dependencies of the ice sheet model for the warm period of the Late Pliocene using 30 different models (Dolan et al., 2012). Figure 1 provides a visual comparison of the modern and LP ice sheet extent. LP GrIS reconstruction is provided for PlioMIP2 Haywood et al. (2016a) and based on 30 modelling results from the PLISMIP project Dolan et al. (2012). Power and Zhang (2024) provides more detail, including spatial configuration of the LP GrIS and associated climatic impacts of modifying the GrIS in the polar Northern Hemisphere.

~~The PlioMIP ice sheet mask was interpolated onto the grid of~~ In our sensitivity experiments, the LP ice-sheet masks were interpolated to the EC-Earth ~~'s atmospheric component, IFS ,~~ IFS grid and substituted into the ~~snow depth variable of the initial condition file. IFS does not have a specific variable for ice sheets, therefore, altering the snow depth provides only a change in the ice sheet extent, being ice sheetsthe~~ initial-condition referred to as the snow-depth field. In IFS, ice-sheet presence is defined as grid cells with snow depth > 10 meter. By altering this field, we therefore reclassify those cells as exposed land or ocean in the LP experiments. The snow scheme in EC-Earth3 (based on ECMWF's HTESSEL land surface model) treats snow as perennial when snow depth exceeds a threshold 0.5 meter of water equivalent, assigning a fixed high albedo and preventing further accumulation, effectively acting as a proxy for ice sheets. When snow depth is below this threshold, snow is considered seasonal and surface albedo is calculated as a weighted average between snow albedo and underlying surface albedo, reflecting seasonal snow cover variability (Döscher et al., 2022; Balsamo et al., 2009). In our experiments, the AIS orography is retained, but in regions where snow depth ~~exceeds 10 metres. To solely focus on climatic feedbacks resulting from change of AIS and~~

~~GrIS; albedovalues and ice sheet orography were not modified, and accompanying freshwater hosing experiments to account for~~
~~meltwater from ice sheet change were not performed. With these exclusions, we aim to create idealised sensitivity experiments.~~ falls below the perennial threshold, seasonal snow processes dominate, allowing accumulation and melt with seasonally varying albedo. All other initial and boundary conditions were held fixed at PI values, including the prescribed surface albedo fields, orography/elevation, GHG concentrations, aerosol fields, ocean boundaries, soil and vegetation distribution, together with their modified albedo properties. Additionally, no freshwater hosing was applied.

This experimental design therefore isolates the climatic response to the geometric removal of ice cover under fixed pre-industrial albedo and topography. Areas that are ice-covered in PI but ice-free in LP retain the model's default PI surface properties for that grid cell type (bare land or ocean), rather than adopting LP specific albedo or vegetation reconstructions. This design allows us to focus on the first-order radiative effect. By doing so, we isolate the radiative effect of land ice loss, how the change in surface reflectivity influences the local and regional energy balance, and the resulting dynamical response, including how these changes affect atmospheric circulation, wind patterns and ocean feedbacks within the model framework. This controlled experimental design avoids confounding influences from additional forcings such as changes in vegetation, soil moisture, or orography, which may otherwise obscure the direct climatic impact of ice retreat. In this way, the experiment acts as a valuable idealized sensitivity test that serves as a baseline for understanding the isolated role of ice sheet retreat on Southern Hemisphere climate dynamics.

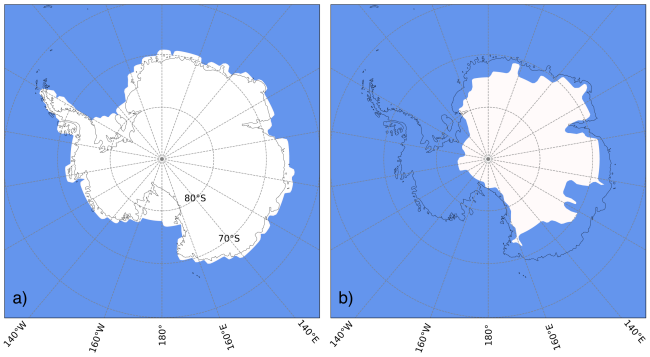

~~Comparison of the modern and LP Antarctic ice sheet extent as provided by the PLISMIP project.~~

Figure 1. Comparison of the a) modern and b) LP Antarctic ice sheet extent in white, as provided by the PLISMIP project. Superimposed is the modern coastline of the Antarctic continent.

~~These simulations are part of the Pliocene for Future (P4F)Tier 2 experiments (Haywood et al., 2016a), which has been proposed for the second phase of the Pliocene Model Intercomparison Project (PlioMIP2) and will be included in the new PlioMIP3 experiment list. The reliability of the Antarctic ice sheet extent is further supported by the results of the PLISMIP results, which evaluated the dependencies of the ice sheet model for the warm period of the mid-Pliocene using 30 different models (Dolan et al., 2012). To ensure consistency across all simulations, modern vegetation, as simulated for the year 1850~~

CE, was fixed using the off-line LPJ-GUESS dynamic vegetation model (Chen et al., 2021). Each simulation spans a minimum of 1450 years, with the final 200 years of model output used for analysis of the mean state. The pre-industrial configuration (E280) serves as the PI control experiment for comparison.

3 The polar Southern Hemisphere response to increased CO_2 and LP ice sheets

The interactions between the atmosphere, cryosphere and ocean are crucial in understanding the influence of increased atmospheric CO_2 concentrations and reduced ice sheet extent on climate feedbacks in the polar Southern Hemisphere.

3.1 Changes to temperature, albedo and sea ice concentration

In the E400 scenario (400 ppm CO_2, relative to E280), the average Antarctic surface air temperature rises by 2.51°C. The warming is most pronounced in two specific hotspots - Weddell and Ross regions that we refer to as *"hotspots"*, the Weddell (50°W, 75°S) and Ross (160°W, 73°S) seas, with temperatures increasing up to 6°C in the Weddell Sea (50°W, 75°S) and and by 5°C in the Ross Sea (160°W, 73°S) (figure 2a). Changes to albedo (Figure 2c) are primarily confined to these two regions, with the most significant decrease (up to 20%) occurring in the Weddell Sea, extending between the from coastline to 60°S, and clustered to the coastline moving eastwardWeddell gyre. A smaller area of albedo decline (10%) is observed west of the Ross Sea. Sea ice loss replicates these patterns surrounding the hotspots*hotspots*. Largest sea ice decline occurs to the east of the Weddell Sea (Figure 2e) and clustered to the coastline moving eastward, and a smaller area of sea ice loss found west of the Ross Sea. More moderate warming occurs across the majority of the remaining area, with generally less than 2°C increase over the interior of Antarctica and less than 1°C at the periphery of east Antarctica. This is accompanied by close to zero changes in albedo. A localised cooling of 1–2°C is observed in the southern ocean between 160°W-160°E, 62°S, where a small loss in albedo is also displayed (Figure 2c).

With In contrast, with LP ice sheet extent (Ei400 relative to E280), warming is much greater than in E400; Antarctic , with the near-surface air temperature increases over Antarctica increasing by an average of 9.49°C. The warming hotspots *hotspots* shift further inland, with temperatures rising by over 17°C inland from the Ross Sea (180°–155°W, 81°–83°S) and up to 16°C inland from the Weddell Sea (20°–35°W, 81°–83°S) (Figure ??2b). The Ross and Weddell Seas themselves experience warming of up to 12°C and 13°C, respectively. The most substantial albedo declines also occur at these inland hotspots;, with a greater than 50% decline inland of the Ross Sea, whilst the Ross Sea itself experiences 30% decrease. There is an albedo reduction of 40-50% inland of the Weddell Sea, which extends into the Weddell Sea itself (Figure 2d). Sea ice losses are, consequently most drastic in these locations, with over 65% decline in the Weddel and 60% in the Ross Sea. High Moreover, extensive areas of sea ice loss are observed extending eastward from the Weddell Sea and westward from the Ross Sea.

Over the interior of Antarctica, warming reaches 11–12°C, decreasing towards the eastern coastline where temperatures increase by 6–7°C. In Ei400, albedo changes are not confined to regions affected by ice sheet change and there is an overall albedo decline of 20% across the Antarctic interior, with decreasing severity toward the eastern coastline. There is a small hotspot *hotspot* showing pronounced loss of 30-40% on the east coast (60°–70°E, 75°S). Additionally, albedo decreases of up

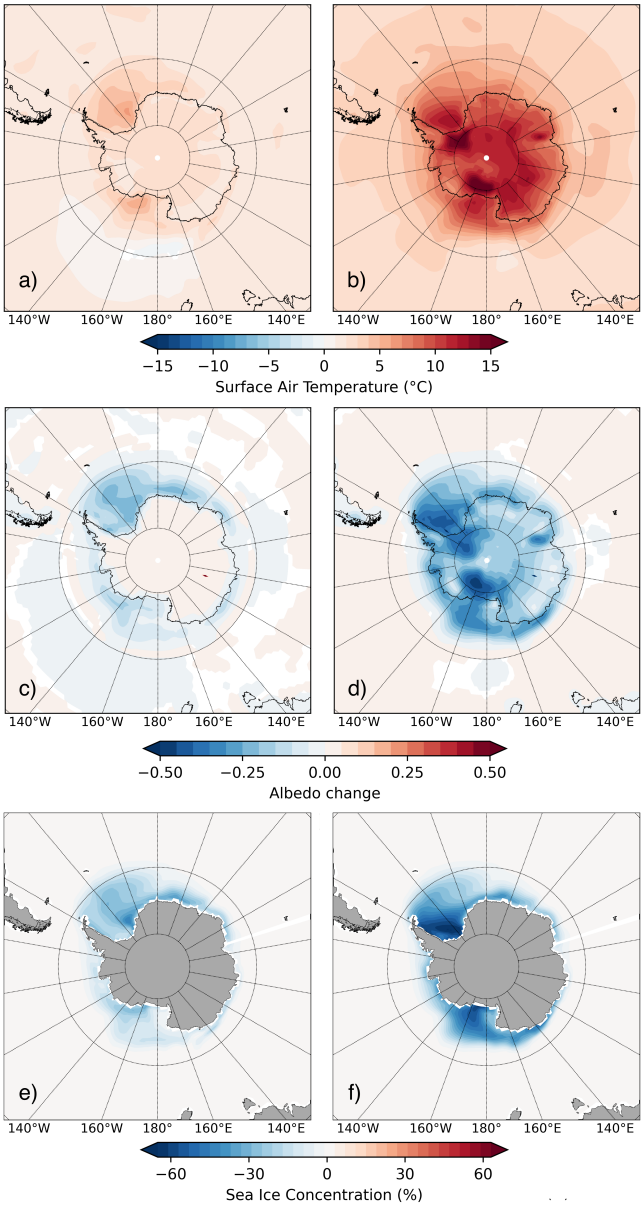

Figure 2. Temperature, Albedo and Sea Ice Concentration (SIC) variables from the only increased CO_2 level experiment and combined CO_2 and LP Ice Sheet extent, compared with the PI control. a) E400-E280 surface air temperature, b) Ei400-E280 surface air temperature, c) E400-E280 albedo, d) Ei400-E280 albedo, e) E400-E280 ~~Sicone~~SIC, f) Ei400-E280 ~~Sicone~~SIC. Only results statistically significant at the 95% confidence level are displayed.

to 30% are observed along the coastline at 0°–10°E and 140°–160°E. ~~These widespread albedo reductions are~~ This widespread

albedo reduction is a result of the interplay of climate feedbacks ~~, with~~ that likely include changes in cloud cover, atmospheric temperature and moisture transport influencing the radiation balance and surface reflectivity.

3.2 Changes to regional atmospheric circulation patterns

As the surface temperature rises due to the abrupt change in radiative forcing applied through our experiments, the subsequent shifts in ~~the~~ climate create significant feedbacks that can influence large-scale atmospheric circulation, particularly the Southern Annular Mode (SAM). SAM is the leading mode of atmospheric variability in the Southern Hemisphere, characterised by fluctuations in the strength and position of the westerly winds encircling Antarctica (Marshall, 2003). It has a large influence on pSH climate, ~~sea ice cover and ocean circulation~~as the wind regimes over this region modulate sea ice and deep water formation, as well as other climate pattens (Morioka et al., 2024). Therefore, understanding how it responds to increased CO_2 concentrations and ice sheet changes is vital. Here we derive SAM mean state ~~anomaly~~ of the sensitivity experiments ~~in relation to PI~~ (Figure 3a, b, and c) by applying Empirical Orthogonal Functions (EOF) to the Sea Level Pressure (SLP) field and extracting its first mode. SAM variability in the form of a timeseries spanning the last 200 simulation years (Figure ~~??~~4) was extracted through the first Principal Component of the EOF (PC1) ~~, standardizedusing a Savitzky-Golay filter~~and standardized.

~~In the control scenario, SAM (Figure ??a) displays a relatively well balanced variability, oscillating between positive and negative phases, but with marginally more occurrences of positive SAM phases during the period. This is recognised with the spatial pattern of EOF1, aligning with a more positive SAM.~~

~~Under increased CO_2 (E400) there are more positive SAM events and fewer strong negative SAM phases, occurring over the time period compared to control, (Figure ??b) . Spatially, a slightly stronger and more persistent SAM pattern is evident (Figure 3a) , with an increase in pressure variability north of 60°S, consistent with stronger fluctuations in the westerly jet (~~

	Median	**Std Dev**	**Kurtosis**	**Positive** (> 0)	**Negative** (< 0)	**Extreme Positive** ($> +1\sigma$)	**Extreme Negative** ($< -1\sigma$)
E280	0.040	43983.738	0.086	51.9%	48.1%	15.589	15.630
E400	-0.071	44550.820	0.217	46.7%	53.3%	15.962	14.712
Ei400	-0.035	45612.121	0.246	48.6%	51.4%	15.133	15.547

Table 2. Summary statistics - mean, variability (std), kurtosis, occurrence percentages of positive/negative and extreme events, describing the temporal behavior of the first principal component (PC1) representing the SAM index in each experiment. Standard Deviation and kurtosis are based on non-normalised data, all others on normalised data.

In E280, Figure ~~3c), the primary characteristic of a SAM~~ 3a reveals an atmospheric structure characteristic of a positive ~~phase. Pressure variability decreases south of 65~~SAM phase, with lower than normal SLP over Antarctica (90-60°~~S, meaning a more stable polar vortex and reduced pressure fluctuations (Figure 3a).~~

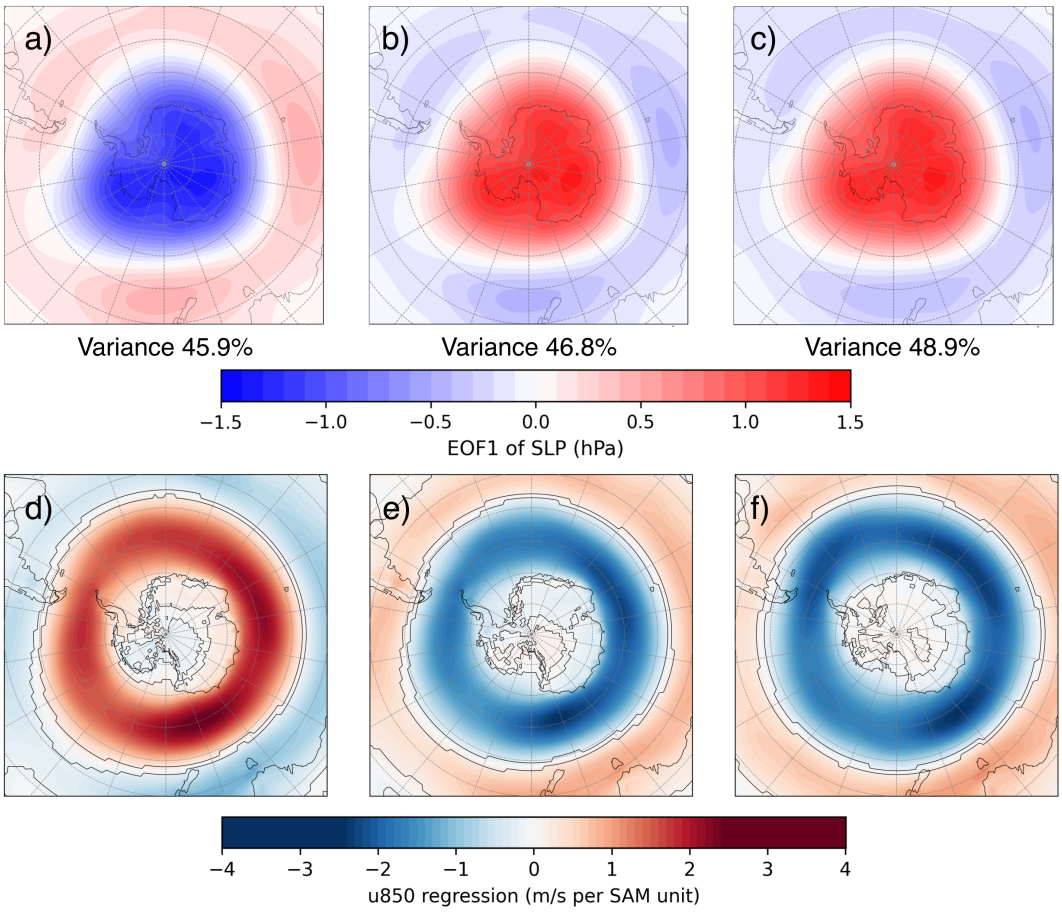

Figure 3. ~~Anomaly (experiment - E280) of the (a,b)~~ The Southern Annular Mode mean state as the first EOF of the SLP in hPa~~; and (c~~, ~~d~~for the a) ~~Eastward Wind speed at 850 hPa~~PI Control, b) E400 and c) Ei400 experiments with % of variance explained by EOF1 notated for each. Regression of the austral summer (DJF) 850hPa zonal wind onto the leading SAM principal component for d) E280, e) E400 and f) Ei400~~experiments~~. Colors indicate the regression coefficient per SAM unit). Black contours denote statistically significant values ($p < 0.05$). Austral summer (DJF) is used as the SAM signal is typically strongest during this period, ~~respectively~~with the stratospheric polar vortex remaining strong and the westerly jet is well-defined.

S) and higher than normal SLP in the mid-latitudes. Regression of austral summer (December-January-February; DJF) 850 hPa zonal wind onto the leading SAM principal component (PC1) shows the strengthening of mid-latitude westerlies, whilst easterlies strengthen to the north of the Antarctic Polar Front (APF; Figure 3d), reflecting the poleward shift of the mid-latitude westerly jet during positive SAM phases (Marshall, 2003). The PC1 reiterates (Figure 4a) the overall positive phase, with a slight positive central tendency (median 0.04) and marginally more positive months than negative (Table 2). A more positive SAM phase is typically associated with cooler temperatures over Antarctica in summer, ~~as~~ such as those established in the

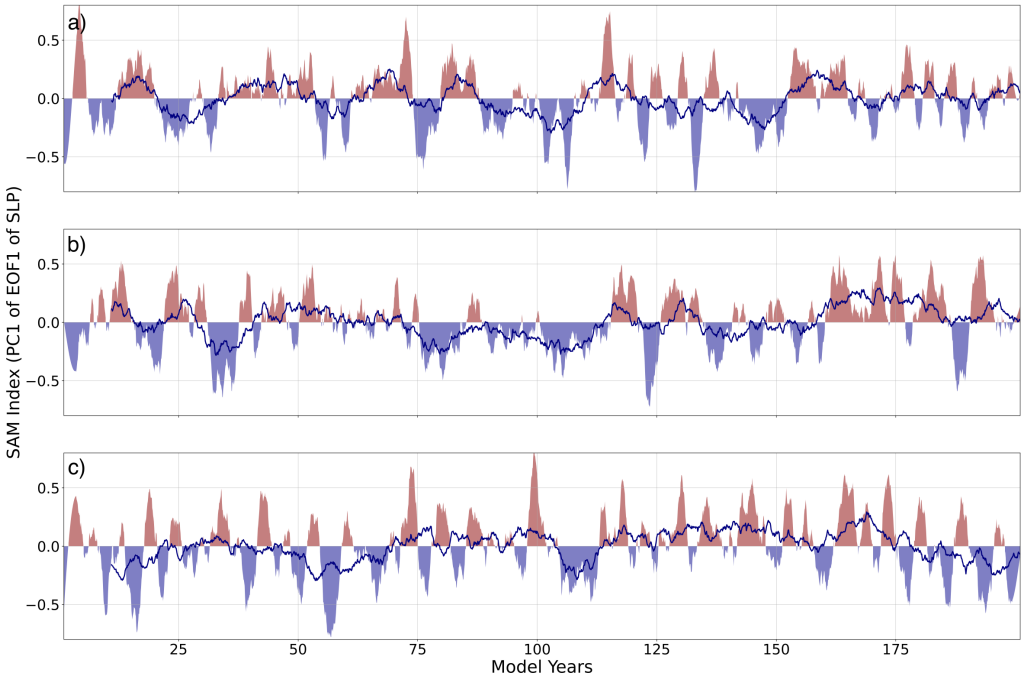

Figure 4. Time series of the Southern Annular Mode (SAM) index for a) E280, b) E400 and c) Ei400 experiments, calculated as the standardized principal component (PC1) of the leading empirical orthogonal function (EOF1) of monthly mean sea-level pressure (SLP) south of 20°S. A Savitzky Golay filter with window of 61 is applied, smoothing the index over 5 years either side, overlaid is a 10 year running mean.

E280 simulation, as stronger westerly winds act as a barrier to warm air transport from lower latitudes ~~. However, despite the shift toward a more positive SAM in~~ (Thompson et al., 2011).

Under increased CO_2 forcing (E400~~, Antarctica still experiences warming (Figure 2a). This is likely due to the comparable forcing of the SAM index is small compared to the direct radiative forcing from increased CO_2. Whilst the cooling effect of a positive~~), there is a reversal in EOF polarity. Higher than normal SLP is present over Antarctica and lower than normal SLP in the mid-latitudes (Figure 3b), indicative of a negative SAM phase. Mid-latitude Southern Ocean winds show strong negative anomalies (Figure 3e), indicating an equatorial shift of the westerlies, thereby reaffirming the negative SAM phase. The PC1 timeseries (Figure 4b) has a slight negative central tendency (median -0.07) and more negative months than positive. A negative SAM phase is ~~strongest in summer, CO_2-induced warming occurs throughout the year, leading to a net temperature increase despite the SAM shift. Plus, sea ice declines may enhance warming that SAM cooling may not be able to compete with~~associated with higher air temperatures across Antarctica, and often leads to reduced sea ice formation that is triggered by katabatic winds in the pSH (Doddridge and Marshall, 2017) . This in turn, reduces the upwelling of cold, deep ocean water onto the Antarctic continental shelf, further reinforcing this negative feedback.

Timeseries of the Southern Annular Mode index derived from a Principal Component Analysis (PC1) for the a) E280, b) E400 and c) Ei400 experiments. The timeseries displays the last 200-year of the quasi-equilibrated simulations. The SAM index is filtered using a Savitzky-Golay filter.

Combining CO_2 with LP ice sheet extent, results in a greater variability of the SAM (Figure ??c), rather than a shift to a particular state. The distribution of events within the equilibrium period is broader, meaning both more extreme positive and negative SAM phases than control or E400. This indicates rather than a shift to one particular state, a more chaotic and less stable SAM pattern has emerged. EOF1 spatial pattern shows large increases in pressure variability from 60°S to the Antarctic coastline, (Figure 3b), supporting enhanced pressure fluctuations and a less stable atmospheric pattern. This change to the SAM stability is driven by a weakening of the SAM dominant control - the westerly jet (Figure 3d). same large-scale atmospheric structure as in E400, characterised by a negative SAM phase (Figure 3c). The PC1 timeseries (Figure 4c), however, demonstrates a behavior closer to neutral in Ei400 than in E400, with a very small negative median (-0.03) and the most even split of negative to positive months out of the three experiments (Table 2). Additionally, Ei400 displays the largest raw variability (in units of the original PC1), potentially indicating a more chaotic and less stable SAM pattern.

3.3 Sea Surface and deep water formation sensitivity to modified boundary conditions

Anomaly of the Sea Surface Temperature (°C) in a) E400 and b) Ei400 in relation to PI

Anomaly of the Sea Surface Salinity (PSU) in a) E400 and b) Ei400 in relation to PI

Changing the AIS and GrIS to LP extents has As evidenced in the previous section, the modified boundary conditions that were imposed in our experiments have significant implications for processes occurring in the near-surface atmosphere. Consequently, the sea surface and deep waters of the polar Southern Hemisphere. At the surface (0-10 meters), the ocean temperature does not reproduce the same warming in the hotspot regions as observed in and the ocean interior of the pSH are also affected. In E400, where we solely increase the atmospheric CO_2 concentration, the surface ocean exhibits similar warming patterns as the atmosphere (Figure 2a. Rather than a more pronounced warming in the Weddel and Ross Seas, increasing the atmospheric CO_2 concentration to 400 ppmv results in), albeit at a much lower magnitude. Figure 5a shows an overall warming along the path of the Antarctic Circumpolar Current (ACC), particularly within 45-55°°S and through the Brazil-Malvinas Confluence (BMC)(, as well as warming hotspots in the Weddell and Ross Seas, that are advected eastward through the ACC. Additionally, the Pacific upper ocean cooling exhibited in Figure 5a). Under elevated CO_2 and LP ice sheet extentis in close agreement both in magnitude and in location with the region where atmospheric cooling occurs. In Ei400, sea surface warming (Figure 5b) agrees even more consistently with air surface temperature change . The warm hotspot pattern seen at the change in near-surface atmospheric temperature (Figure 2b). The warming hotspots confined to the Ross and Weddell Seas, and Adelie coast is now evident, with also remain, with the same pattern of eastward advection of warm waters as in E400, although with SST increasing up to 5°C in the Weddell Sea. A warmer circle related to the zonal heat transport promoted by the ACC around Antarctica within the latitudinal belt of 45-55°S is also evident.

With warming of the Earth's surface leading to an extensive sea-ice melt (Figures 2e and f), the surface layer of the Southern Ocean undergoes substantial freshening around the Sea Ice Zone (SIZ), that is highly sectorised. In E400 , the waters encircling

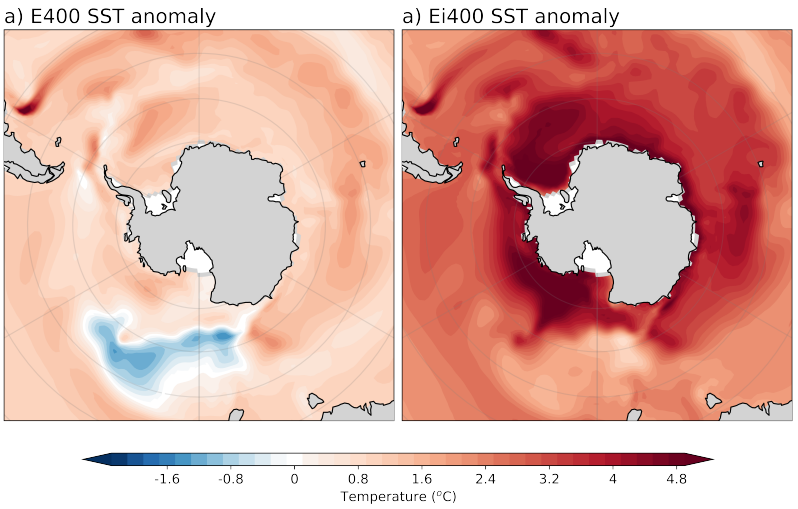

Figure 5. Anomaly of the Sea Surface Temperature (°C) in a) E400 and b) Ei400 in relation to E280. Only results statistically significant at the 95% confidence level are displayed.

~~Antarctica undergo an overall decrease in sea surface salinity~~ (Figure 6a)~~. Surface salinisation occurs in the~~ , the Bellinghausen and Davis Seas exhibit the highest freshening, whereas the region encircling the APF (north of 55˚S), the wind-driven outcrop of the Circumpolar Deep Water (CDW) ~~associated with~~ in the Weddell gyre~~(located north of the Weddell Sea) and to a smaller extent the region associated with the Ross gyre. Salinisation of the upper ocean is also observed around the ACC path north of 55ºS. Under~~ , and some parts of the Ross Sea exhibit upper ocean salinization. Conversely, with the stronger reduction in sea ice concentration that is imposed by reducing the ice sheet extent (Ei400~~conditions, a decrease in salinisation is evident across the pSH (Figure 6~~), the surface freshening of the Southern Ocean is amplified (Figure 6b) while the salinization in the outcrop region of the CDW, Ross Sea and outside the APF remains, albeit at a much reduced magnitude.

The combined effect of upper ocean warming and freshening with weaker wind regimes within the APF (Figures 3e and f) also affect the distribution of these thermohaline properties in the water column. Within the limit of the polar Southern Hemisphere, at 60°S, both E400 and Ei400 experiments exhibit the development of a fresh cap in the upper ocean that, by itself increases the stratification of the water column (Figures 7a and b) with respect to the pre-industrial climatology. As the westerlies weaken concomitantly, the stratification is sustained throughout the simulation, which further isolates the surface ocean. Moving down from the upper ocean, in E400 (Figure 7a), the entire water column exhibits an uniform warming and salinisation during runtime that is consistent with the higher sectorisation of areas that experience cooling (warming) and freshening (salinisation).

In contrast, in Ei400 (Figure 7b), ~~with waters close to the landmass undergoing the greatest decline in salinity. The only areas of salinisation are the wind-driven outcrop of the CDW associated with the Weddell and Ross Gyres, and~~ however, the upper ocean experience warming and freshening, whereas the subsurface undergo warming and salinisation down to the intermediate

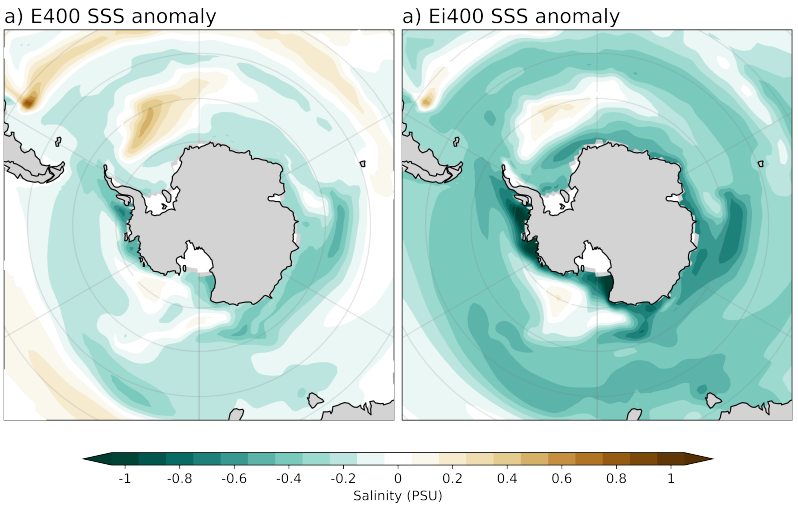

Figure 6. Anomaly of the Sea Surface Salinity (PSU) in a) E400 and b) Ei400 in relation to E280. Only results statistically significant at the 95% confidence level are displayed.

layer (∼ 1000 m). This indicates an increase in stratification and a subsequent isolation of the ocean interior that allows for its stronger salinisation in comparison to E400, especially at deep and abyssal depths. This likely occurs as a combined effect of the ~~ACC path, although magnitudes are less than under E400.~~ stronger stabilisation of the upper ocean, further reinforced by even weaker westerlies (Figure 3f) and the entrainment of salty water masses through the intermediate layers of the Southern Ocean. Additionally, the abrupt forcing that is introduced by reducing the ice sheet extent in Ei400 results in an initial cooling of the ocean interior of about 3°C, that offsets the degree of deep ocean warming in this simulation, when compared to E400. Therefore, in comparison to the pattern revealed in Figure 7a, in Ei400, the Southern Ocean interior (surface) undergoes more salinisation (freshening) and less (more) warming.

~~The CDW, represented by the clockwise circulation south of 55°S in Figure 8, is successively weakened under first elevated CO_2 and CO_2 forcing combined with changed ice sheet extent. The~~ As the changes in the sea surface temperature and salinity, that are amplified in Ei400 with respect to E400, impose contrasting effects in the ocean interior, the Southern Ocean Meridional Overturning Circulation (SMOC) ~~also demonstrates a weakening~~ undergoes a major shift (Figure 8), particularly with respect to the strength of the AABW, ~~from maximum combined strength in the subtropical ocean basins of 8 Sv, as opposed to barely reaching~~ which is essential for the ventilation of the global ocean (Orsi et al., 1999). Firstly, the SMOC reveals two major cells in E280: a clockwise cell that represents the northward flow of surface waters and the return flow of deep and intermediate waters that upwell at around 60°S, and an anticlockwise cell that represents the northward flow of the AABW towards Indo-Pacific and Atlantic basins (Talley et al., 2016). In E400, the clockwise cell deepens and the AABW is significantly weakened from 8-2 Sv. In Ei400, on the other hand, the clockwise cell weakens and shoals, while the AABW

~~Southern Ocean MOC for the a) E280, b) E400, and c) Ei400 experiments averaged over the last 200 years of the simulation~~

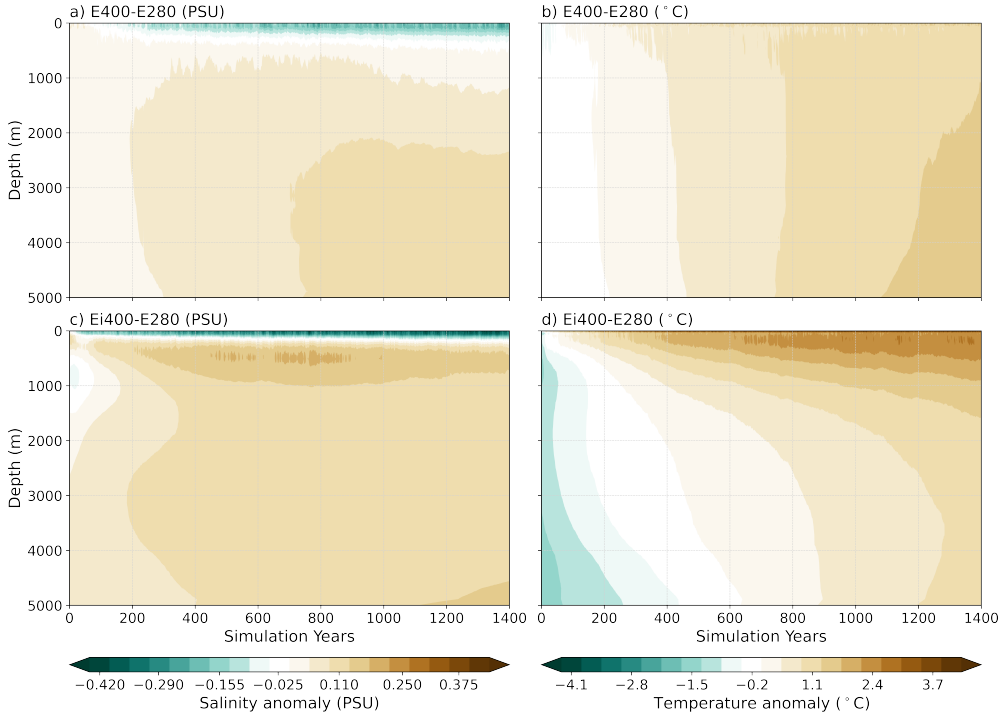

Figure 7. Hovmöller diagrams of salinity (a, b) and temperature (b, d) anomalies at 60°S, relative to E280 average at the same latitude, for E400 (a, b) and Ei400 (c, d).

exhibit a slight strengthening of about 2 Sv~~in E400 and 4 Sv in Ei400. To further investigate AABW formation during runtime, we derive the time series of~~ .

Considering the mean state of the last 200 simulation years, we therefore see that the AABW undergoes extensive weakening in both sensitivity simulations. Such sustained weakening is consistent with the picture of freshening and warming of the upper ocean displayed in Figure 7, but not completely consistent with the picture of salinisation of the deep ocean. To evaluate the strength and variability of AABW formation in our experiments during runtime and gain more insights into the overall state of abyssal overturning in the Southern Ocean, we derived an AABW index that consists of the ~~AABW index (Figure ??). This index was calculated by deriving the~~ absolute value of the minimum ~~global streamfunction of the entire pSH domain, however below 500m~~ overturning south of 60°S, and below 500 m depth (adapted from Zhang et al. (2019)~~to avoid incorporating surface overturning in our index.~~

~~Time series of the Antarctic Bottom Water formation index for experiments E280, E400 and Ei400, calculated as the absolute value of the minimum global streamfunction of the pSH domain (60-90°S) and below 500 m depth (adapted from Zhang et al. (2019)).~~

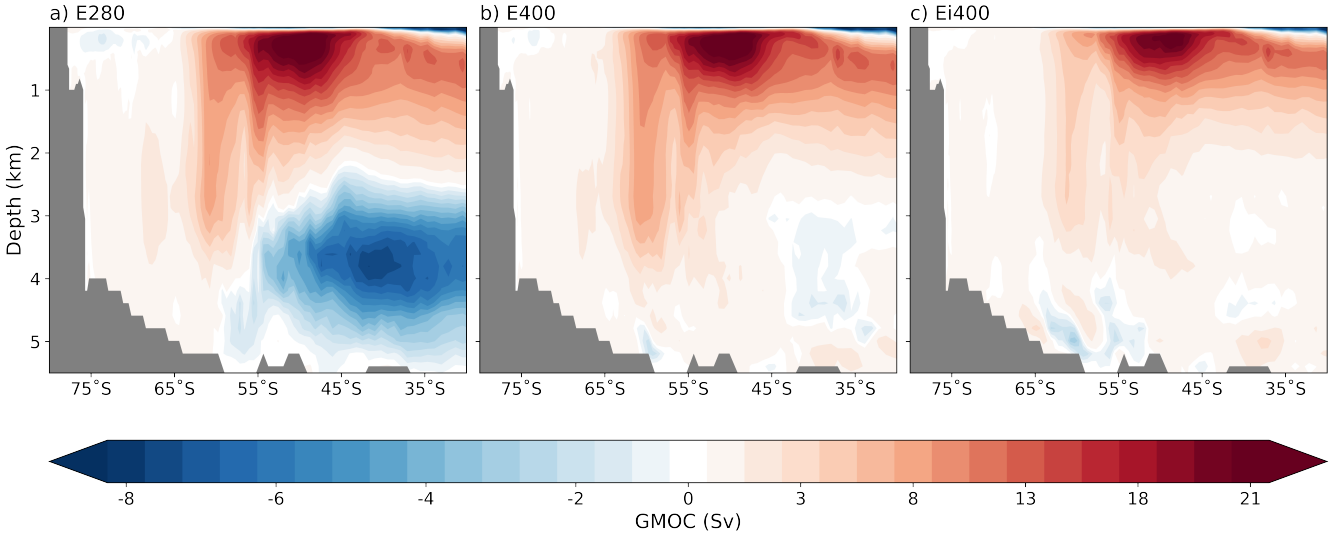

Figure 8. Southern Ocean MOC for the a) E280, b) E400, and c) Ei400 experiments averaged over the last 200 years of the simulation

~~Figure 9reveals thatthe variability of AABW is strongly decreased in both~~). Please note that we exclude the upper 500 m from the index to isolate the water column comprising the subsurface to abyssal layers from the upper ocean and avoid capturing its high frequency variability. The AABW index (Figure 9), shows that, even though Figures 8b and c indicate a similar pattern of AABW weakening in both sensitivity experiments, the evolution of the AABW strength shows a sustained weakening in E400 ~~and Ei400 experimentsin relation to the E280 experiment and there is an initial AABW weakening of approximately 1 Sv by year 700 of the simulation. AABW trends diverge in the later stages of the simulation. In the E400, AABW continues to weaken, whereas~~ and a partial recovery in Ei400, ~~it begins to recover after~~ particularly after simulation year 700. ~~This recovery suggests that the LP ice sheetstrigger a compensatory mechanism~~Additionally, in both sensitivity experiments, the variability of the AABW is significantly reduced with respect to E280. Such behaviour indicates that enhancing the atmospheric CO_2 concentrations, accompanied by massively reducing the extent of ice sheets, trigger compensatory mechanisms to the initial AABW suppression, likely involving ~~the~~ salinisation of the ~~Southern Ocean at deeper levels, which enhances AABW strength and counteracts the initial suppression. Figure 7g, confirms this hypothesis, as the Southern Ocean experiences increase in salinity during runtime at 3 km in the~~ deep and bottom ocean, as suggested in Figure 7.

Furthermore, as the AABW formation is a complex process that is not yet fully understood, and receives contribution from other masses formed in the Southern Ocean, particularly in the deep ocean (Pardo et al., 2012), the insights gained from Figures 7, 8 and 9, indicate that the underlying mechanism for the partial recovery of the AABW in Ei400 ~~experiment.~~ is a combination of the changes in salinity and temperature that occur in the water column, isolated through the weakened wind regime (Figure 3f), and the interplay between the water masses in the Southern Ocean that are directly affected by these changes. The overall change in water mass density and thermohaline properties can be easily visualized through a temperature-salinity (TS) diagram (Figure 10). In the figure, we highlight major water masses that are formed in the Southern Ocean and directly contribute, or

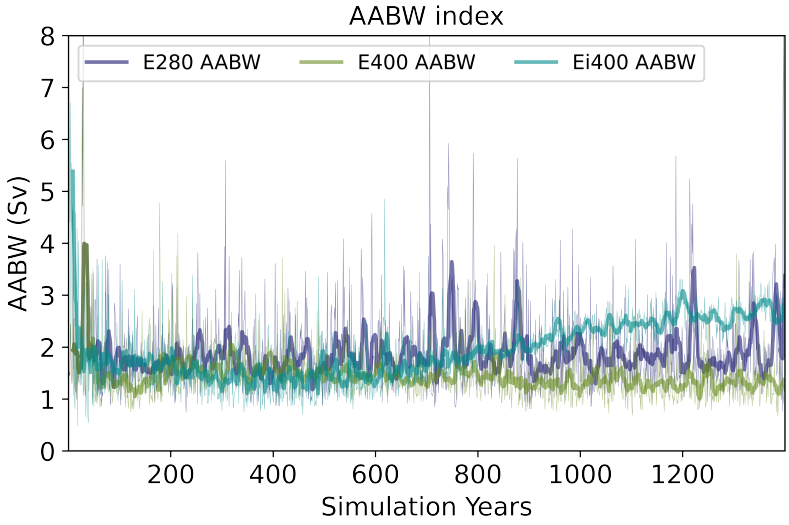

Figure 9. Time series of the Antarctic Bottom Water formation index for experiments E280, E400 and Ei400, calculated as the absolute value of the minimum global streamfunction of the pSH domain (60-90°S and below 500 m depth (adapted from Zhang et al. (2019)).

are the main product of deep water formation that is exported to the global ocean, including: Antarctic Surface Water (AASW), Antarctic Intermediate Water (AAIW), Circumpolar Deep Water (CDW), High Salinity Shelf Water (HSSW), and Antarctic Bottom Water (AABW). In this sense, AASW, CDW and HSSW are contributors to AABW formation (Orsi et al., 1999), whereas AAIW does not play a direct role in AABW formation but is directly impacted by the nature of our experiments (Pardo et al., 2012; Talley et al., 2016). A detailed description of their thermohaline properties in each simulation as well as density levels where they are formed is detailed in Table 3.

~~Analysing the temperature and salinity through the surface, intermediate,~~ Upon comparing E400 and ~~deeper levels of the water column over time, there is an increase of ocean temperature of 1.5°C occurring at 1, 2 and 3 km depths, relative to the beginning of the simulation (Figures 7b~~Ei400 with E280, all water masses displayed in Figure 10 are formed at warmer temperatures. This reflects the overall warming of the water column that is observed in Figures 7b and d. Conversely, the evolution of salinity during runtime in Figures 7a and c, display a contrasting pattern within the entire water column, that is also reflected in the overall lighter densities that are occupied by these water masses. Specifically, the AASW is the lightest water mass ($\gamma_\theta < 27 kgm^{-3}$) displaye in Figure 10, that loses buoyancy during winter through brine rejection and is transformed into the HSSW ($\gamma_\theta > 27 kgm^{-3}$), which subsequently descends through the water column and feeds the AABW. On the other hand, the CDW, brought through the Meridional Overturning Circulation is an important water mass that, via diapycnal mixing with AASW and HSSW, directly contributes to AABW formation (Pardo et al., 2012). In E400 (Figure 10b), the AABW is contracted, and the AASW and HSSW become substantially fresher and lighter, with respect to E280. This indicates a reduced dense shelf overflow that ultimately weakens the AABW formation. As CDW becomes saltier and warmer to a degree that

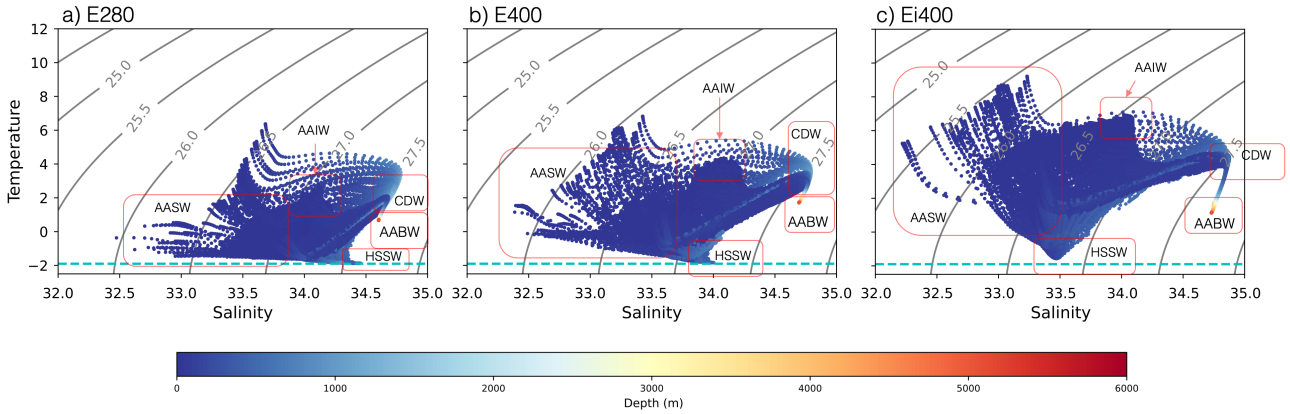

Figure 10. ~~Time series~~ Potential temperature (θ)–salinity (T–S) diagrams of the ~~salinity~~ Southern Ocean for a) E280, b) E400 , and ~~temperature of~~ c) Ei400 , averaged over the last 200 simulation years. Gray solid lines show the isopycnals of 24.5-28 kgm^{-3}. Please note that the ~~pSH domain~~ color scheme refers to the depth at which water masses are formed in the Southern Ocean. The cyan dashed horizontal line shows the the surface freezing point of seawater (~~60-90°S~~1.8°C)~~at~~ . Major water masses are labeled as: Antarctic Surface Water (~~a,b~~AASW)~~surface~~, Antarctic Intermediate Water (~~c,d~~AAIW)~~1km~~, Circumpolar Deep Water (~~e~~CDW), ~~f~~High Salinity Shelf Water (HSSW)~~2km~~ , and Antarctic Bottom Water (~~g,h~~AABW)~~3km depths~~.

does not modify its density and the upwelling induced by the westerlies is not increased during runtime, its entrainment into the Southern Ocean is not able to destabilize the stratification towards promoting more deep water formation.

Conversely, in Ei400~~than in~~ , the AABW is expanded, becoming denser and saltier, while maintaining its temperature in comparison to E280. Additionally, the change in thermohaline properties and density of the AASW and HSSW are amplified with respect to E400~~. The surface layers show substantial freshening, whilst deeper layers undergo initial salinisation for the first 700~~ , but the CDW becomes saltier, which suggests enhanced entrainment of saltier waters into the Antarctic shelf and subsequent increase the abyssal salinity. These processes combined justify the partial recovery of the AABW towards the end of the Ei400 simulation, even with relatively stable conditions in the upper ocean. In summary, freshening of the upper ocean induces increased stratification in both experiments that reduces the export of dense shelf water to the bottom of the ocean and results in an overall AABW supression in the first years of the ~~simulation (Figures 7 a, c, e and g), followed by a transition to freshening, except for 3 km~~E400 and Ei400 experiments. However, reducing the ice sheets imposes an extra freshening and warming of the upper ocean that further isolates the ocean interior, while the subsurface and deeper ocean undergo a more intense salinisation that incurs in increased AABW formation, not necessarily induced by the change in ice sheet itself but by possible teleconnections with other ocean basins further North.

Table 3. Thermohaline Properties and Density location of Southern Ocean water masses highlighted in Figure 10. Density is potential density anomaly γ_θ (kgm^{-3}) relative to 1000 kgm^{-3}. The order of properties in the column representing the experiments is: Salinity (S; PSU), Potential temperature (°C),and Density (γ_θ)

Water mass	E280	E400	Ei400
AABW	$S \sim 34.6$, ~~d, f and h). The degree of warming is about 2°C higher~~ $\theta \sim 1$, $\gamma_\theta \sim 27.7$	$S \sim 34.7, \theta \sim 1.8-2, \gamma_\theta \sim 27.7$	$S \sim 34.8, \theta \sim 1.2-2, \gamma_\theta \sim 27.7$
HSSW	$S \sim 34.3-34.5, \quad \theta \sim -2, \gamma_\theta \sim 27.7$	$S \sim 34, \theta \sim -1.8, \gamma_\theta \sim 27.3$	$S \sim 33.5, \theta \sim -1.6, \gamma_\theta \sim 26.8$
CDW	$S \sim 34.7, \theta \sim 1-2, \gamma_\theta \sim 27.7$	$S \sim 34.8, \theta \sim 1.5, \gamma_\theta \sim 27.7$	$S \sim 34.9, \theta \sim 1.5, \gamma_\theta \sim 27.5$
AAIW	$S \sim 34-34.2, \quad \theta \sim 2-3, \gamma_\theta \sim 27.2$	$S \sim 33.8-34.2, \quad \theta \sim 3-4, \gamma_\theta \sim 27.0$	$S \sim 34, \theta \sim 5-7, \gamma_\theta \sim 26.7$
AASW	$S \sim 33-33.7, \quad \theta \sim -1.8-1, \gamma_\theta \sim 26-27$	$S \sim 32.6-33.5, \quad \theta \sim -1.8-4, \gamma_\theta \sim 25.5-26.7$	$S \sim 32.5-33.2, \quad \theta \sim -1.2-6, \gamma_\theta \sim 25.4-26.5$

4 Discussion

In E400, Antarctic warming is modest overall. Air temperature changes are most pronounced in areas ~~with~~ experiencing sea ice loss and ~~therefore albedodeclines~~associated decline in surface albedo, such as the Weddell Sea. This surface warming flattens the ~~local~~ meridional temperature gradient (Kidston et al., 2011), ~~meaning a weaker local baroclinicity and a reduction in eddy generation and therefore lower pressure varaibility (Figure 3a). The~~ whilst the loss of sea ice ~~contributes to a smoother surface, further weakening baroclinicity and~~ further smooths the surface, suppressing storm development (Screen et al., 2011). ~~Pressure increases around 50–60°S, and the westerly jet strengthens, showing~~ This leads to weaker westerlies, and a shift to a ~~more positive SAM phase . This pattern is consistent with observational and modeling studies, which show a positive~~ negative SAM phase (Figure 3b), which aligns with studies showing a negative SAM in response to ~~greenhouse forcing (Thompson et al., 2005; Marshall, 2003)).~~

~~The stronger westerlies promote more intense~~ regional or seasonal reductions in Antarctic sea ice (Thompson et al., 2005; Marshall, 2003 . The negative SAM contributes stabilizing the upper layer of the Southern ocean (Figure 7) via weaker westerlies that prevent interior mixing (Tamsitt et al., 2017) ~~, encouraging upwelling of colder, yet fresh, deeper water from the abyssal Pacific (aided by topographic constraints imposed by the Macquarie and Pacific-Antarctic Ridges). This contributes to the Pacific cooling evident on both Figure 2 and 5. The~~ and the entrainment of cold, dense waters onto the Antarctic continental shelf. The more extensive sea ice loss ~~here~~ in the Pacific in Ei400, together with weakened wind regimes throughout the APF, drives a

contraction of the seasonal ~~Sea Ice Zone (SIZ)~~ SIZ and reduces Antarctic Divergence (Ramadhan et al., 2022), ~~ultimately meaning a decline in~~ further suppressing the upwelling of warm CDW~~further leading~~ , which further leads to the cooling ~~Pacific hotspot~~confined to the Pacific sector of the Southern Ocean. This behaviour is consistent with current observations (Beadling et al., 2022; Roach et al., 2023; Schmidt et al., 2023). ~~By increasing~~ With increased stratification at deep convection sites ~~, and inhibiting the~~ induced by freshening and warming of the upper ocean, together with the negative SAM phase, vertical mixing required for deep-water formation ~~, the positive phase of the SAM is amplified, intensifying the effects of atmospheric circulation that contribute to regional warming around Antarctica at elevated CO_2 levels~~is limited, which incurs in the suppression fo the AABW.

In Ei400 an intense ~~southern polar~~ pSH warming leads to complex and regionally varying atmospheric responses, agreeing with the consensus from Pliocene Model Intercomparison Project (PlioMIP2), that the influence of a strongly reduced AIS exacerbates the changes induced by a higher CO_2 concentration alone. The strongest warming (up to 16°C) is located over and inland from the Ross and Weddell Seas, ~~also showing~~ an area also showing the largest albedo declines (up to 50%) and significant sea ice losses. ~~Ocean temperatures show widespread warming ; the topographic upwelling enforced by increased Ekman pumping observed in E400 is reduced not only from the decreased Antarctic Divergence but also from reduced overall vertical mixing. Stratification is enhanced due to substantially warmer and fresher surface waters (Figure 6b). The mild freshening of Weddell and RossGyres connects to the weakening of CDW, as both gyres contribute to poleward heat transport and therefore increased sea ice melt, a decreased upwelling and poleward transport of warmer waters.~~

~~It is this freshening and warming of the upper ocean, coupled with sea ice loss, which weakens the AABW. The AABW formation is a process that depends largely on sea-ice dynamics and the interplay between salinity and temperature in~~ The observed inland Antarctic warming pattern dominated by the ~~water column. Under stable conditions, the freshwater fluxes induced by sea-ice melting during summer are balanced by the cold temperatures of the Southern Ocean , whereas the salinity increase induced by brine rejection during sea-ice formation in winter densifies the water column. Such cold dense water mass then moves towards the ocean bottom layer (Silvano et al., 2023). Ocean stratification and reduced brine rejection that happens during sea ice formation and therefore limits AABW formation (Talley, 1993). These results align with the findings of (Sidorenko et al., 2021), where surface buoyancy loss and stronger westerlies over the Southern Ocean inhibit AABW formation and export. These findings suggest that the reduced ice sheets not only amplify surface-driven feedbacks but also initiate deep-ocean processes that partially mitigate the suppression of deep-water formation The Ei400 AABW recovery suggests that LP ice sheets trigger a compensatory mechanism involving the salinisation of the Southern Ocean at deeper levels, to enhance AABW strength and counteract the initial suppression.~~ Ross, Ronne and Amery ice shelves is consistent with physical expectations, as these low-altitude, relatively warm ice shelves act as heat reservoirs, facilitating heat transfer inland. The magnitude of ocean and atmospheric warming displayed in our findings exceed the magnitude suggested for the LP by the PlioMIP2 ensemble (Weiffenbach et al., 2024). However, these large atmospheric and sea surface temperature increases observed is likely influenced by the Southern Ocean bias prevalent in the EC-Earth3 (Döscher et al., 2022) model, as well as by the large spread in the large scale patterns of climate change simulated by the PlioMIP2 ensemble (Haywood et al., 2020). Such uncertainty in the PlioMIP2 ensemble is also a motivation for the development of the third phase of PlioMIP, PlioMIP3

(Haywood et al., 2024), and therefore does not jeopardise neither the quality of the findings displayed here, nor their significance to the scientific community.

~~Regions exhibit different behaviors of SLP variability. Inland from the Weddell Sea, we observe a decrease in SLP variability. This suggests a breakdown of the local temperature gradient, weakening baroclinicity and reducing the strength of transient eddies consistent with E400 and Kidston et al. (2011). Inland from the Ross sea however, pressure variability increases, indicating other regional dynamics such as katabatic winds. Notably, we~~ We also observe adjacent zones of both wind and pressure strengthening and weakening, pointing to disrupted and complex wind regimes around Antarctica, particularly over the continent itself. These non-zonally symmetric changes in both winds and pressure patterns, are consistent with the idea that regional feedbacks and non-linearities emerge once the ice sheet is reduced.

~~Further north, in the circumpolar~~ An example is the weakening of the westerly winds over the Southern Ocean between 50°~~–60~~-60°S~~, there is a weakening of the westerly winds. This~~ . Such weakening aligns with the reduction in the equator-to-pole temperature gradient, which weakens the zonal pressure gradient that drives the westerly jet. In Ei400, the tropical regions warm by 2.32°C, but Antarctica warms by 9.18°C, drastically reducing the meridional temperature contrast from 42.1°C in the control to 37.3°C. A weakening of the gradient leads to a weaker, more meandering jet and a less stable negative SAM pattern (Thompson and Wallace, 2000; Gerber and Vallis, 2007). This ~~explains the observed~~ weakening of the ~~zonal winds and the increase in SAM variability—a signature of a less coherent, more fluctuating SAM state. This weakening of the~~ westerlies also substantially impacts the advection of surface warmer waters by the ACC, and leads to a decrease in formation of coastal polynyas that contribute to sea ice formation and salinisation of the deeper layers of the Southern Ocean (Kusahara et al., 2017).

5 ~~Late Pliocene ice sheets as analogues for future climate~~

Regarding deep water formation, under both elevated atmospheric CO_2 concentrations and LP ice sheet extent, water masses formed in the Southern ocean experience major changes, especially related to AABW, AAIW and CDW formation and export, agreeing with evidence for a weakening of Southern Ocean circulation during past warm geological periods (Noble et al., 2020) . This has been noted in the Miocene (Herold et al., 2012), with reduced southern hemisphere westerlies weakening global overturning circulation and deep water upwelling at the Antarctic divergence, during the Late Pliocene where a highly stratified Southern Ocean weakens the abyssal overturning circulation (Weiffenbach et al., 2024) and in the LIG, where Yeung et al. (2024) demonstrates a subdued ACC, primarily driven by weaker deep-ocean convection due to reduced sea-ice formation leading to changes in meridional density gradients and surface winds. This reoccurrence throughout different paleo periods illustrates that there are numerous key and shared mechanisms responsible for driving changes in the Southern Ocean circulation, that are also displayed in our study.

Specifically with respect to AABW formation, the climatic consequences of the forcing induced through our sensitivity experiments affect sea-ice formation and the development of stratification in the water column. The impacts of elevated CO_2 and LP ice sheet extent directly affect the formation processes of the AABW, a process that depends largely on sea-ice

dynamics and the interplay between salinity and temperature in the water column. Under pre-industrial climate conditions, the water column remains stable during summer through the balance between meltwater input from sea and land ice, and the cold temperatures of the Southern Ocean, whereas the salinity increase induced by brine rejection during sea-ice formation in winter induces formation of cold dense waters towards the ocean bottom layer (Silvano et al., 2023) and contribute AABW formation. However, under enough climatic forcing, the AABW can be suppressed, and its variability can drastically change when comparing to PI conditions. A reduced AABW formation can arise from meltwater input in the Southern Ocean, such as from freshwater pulses from the retreating WAIS following the LIG, as modelled by Menviel et al. (2010), or freshwater discharge from the modern retreat of the AIS in the 21st century, as modelled by Gorte et al. (2023). Alternatively, surface buoyancy loss and stronger westerlies over the Southern Ocean can also inhibit AABW formation and export through induced upwelling of the CDW, thereby reducing dense shelf water formation that is a contributor to AABW. This was noted by Watson et al. (2015) to have occurred during the LGM, when upwelling was shifted further away from the Antarctic coast resulting in the densest waters not being formed at the continental margin, prohibiting AABW formation. Conversely, weaker easterly winds can also reduce sea ice formation at deep convection sites and further inhibit AABW formation via increasing areas of open water, primed for air-sea buoyancy loss and convective overturning, demonstrated by Schmidt et al. (2023) to occur throughout the 20th century. On the other hand, disruption of subpolar westerly winds regimes may also indirectly boost AABW formation, through limiting the accumulation of freshwater around the Southern Ocean and aiding in the process of upper ocean resalinisation after freshwater forcing has ceased Trevena et al. (2008). Changes to AIS topography offer another mechanism by which deep water formation in the Southern ocean can be reduced, illustrated by PlioMIP2 ensemble of experiments incorporating full boundary changes (Haywood et al., 2013). Under these idealized experiments, the lowered AIS elevation reduces the temperature gradient between Antarctica and surrounding air masses, weakening katabatic winds and affecting sea ice production towards restricting dense water formation. Altered AIS topography also impacts other aspects of atmospheric circulation, shifting the Southern Hemisphere westerlies poleward and leading to the before mentioned northward shift in upwelling. Thus, the dynamics that accompany cycles of AABW formation, either through suppression or strengthening are highly complex and not linear through past warm or cold climates. This reinforces the need of continuing to investigate deep water formation in the Southern Ocean under various regimes, as we do here in our study. Ultimately, we show that the isolated effect of albedo-driven warming of the Southern Ocean and melting of sea-ice hinder AABW formation and weakens the SMOC through inducing more stratification in the water column. Our findings therefore parallel the underlying mechanism, as exhibited by other studies, of enhanced upper-ocean stratification suppressing deep convection, without a freshwater forcing or topographic change. Thus, our study shows that reduced ice sheets not only amplify surface-driven feedbacks but also initiate deep-ocean processes that partially mitigate the suppression of deep-water formation, which in itself is a novel perspective, since our experiments in all its particularities, has not been preformed before.

5 Conclusions

There is a notable gap in existing research on the isolated impact of the abrupt removal of large portions of ~~AIS and GrIS~~ ice sheets on climate and ocean circulation. ~~The~~ In this study, we specifically isolate the climatic response to ice sheet retreat to examine its role in driving Antarctic climate dynamics and Southern Ocean circulation, highlighting the Southern Ocean's critical sensitivity to increased atmospheric warming. We utilise the Late Pliocene Age ~~serves~~ as an important analogue of future climate scenarios due to its modern-like atmospheric CO_2 concentrations ~~,~~ and significantly reduced ice sheets~~and ecosystem shifts~~. This paleogeographic framework offers a valuable opportunity to assess climate sensitivity to regional ~~albedo changes. In this study, we specifically isolate the albedo effect of ice sheet reduction to examine its role in driving Antarctic climate dynamics and Southern Ocean circulation. A PlioMIP-conform idealised sensitivity experiment would incorporate the orography changes that would accompany the reduction in ice sheet. Under~~ ice sheet extent changes.

Incorporating the glacial-isostatic driven orographic changes that accompany ice-sheet reduction in both hemispheres would, indubitably, increase the realism of our experiment, as, under future ice sheet loss, the resulting changes in orography ~~that will result~~ are likely to have significant impacts on both the surrounding and global climate and oceans. A large reduction in AIS elevation may lead to strong local warming and a strengthening of poleward energy and momentum transport by baroclinic eddies, whilst the increasing outgoing longwave radiation from the ~~surrounding climate and Southern Ocean. Here, we choose to not include orographical change however. The additional uncertainties from both deriving the parameters needed to modify orography in the model (including adjusting mean orography in the atmospheric component and sub-grid scale parameters such as standard deviation, slope, and angle) and from whether future orographical changes will closely align with those reconstructed for the Late Pliocene, may outweigh the benefits of an idealised sensitivity experiment. Our simulations with isolated PRISM4D ice sheet conditions demonstrate that ice sheets play a critical role in modulating climate feedbacks in response to warming.~~

~~The~~ localised warming, may drive anomalous southward energy transport toward the continent, resulting in cooling elsewhere (Singh et al., 2016). Therefore, the atmospheric and oceanic responses observed in our sensitivity experiments with isolated PRISM4D ice sheet conditions, do not fully reproduce the climate changes seen in more comprehensive modeling studies that incorporate all boundary conditions of the Late Pliocene~~. Nor~~ , nor do they fully match the reconstructed climate based on proxy data (Burls et al., 2017; Haywood et al., 2013, 2016a, 2024). ~~Therefore, point to point comparison needs to be done with caution. Our results do agree with the consensus from Pliocene Model Intercomparison Project (PlioMIP2), that the influence of a strongly reduced AIS exacerbates the changes induced by a higher CO_2 concentration alone. However, Weiffenbach et al. (2024) reported a Southern Ocean SST warming of 2.8°C according to PlioMIP2 ensemble, driven by reduced sea ice cover linked to AIS retreat. This value is less than our average of 4.89°C and agrees better with SST change from AIS melt and elevation change in the Last Interglacial (LIG) of 2°C Hutchinson et al. (2024). The mechanisms we establish, however, are paralleled in both paleo and current work. Our findings of a weakened SMOC, driven by surface layer freshening, and initial salinification at depth, agrees with findings by Yeung et al. (2024), of a weakened deep convection and subsurface warming during the LIG. A reduction in AABW is also established by Gorte et al. (2023). Whilst this experiment models~~

freshwater discharge, the mechanism of enhanced stratification due to freshening suppressing deep convection aligns with our findings here.

6 Conclusions

This study underscores the critical sensitivity of the Southern Ocean to increased atmospheric warming. Current conditions do not yet reflect the full extent of AIS reductionor collapse, as projected in future climate experiments(Roach et al., 2023; Armstrong McKay . However, our results suggest that even under present trends, the ability of the Southern Ocean to ventilate the deep ocean is at significant risk. Furthermore, while we isolate the albedo effect in this study to reduce uncertainties, the exclusion of other climate feedbacks may underestimate the potential catastrophic outcomes of AIS collapseHowever, as our primary objective is to isolate the climatic response to ice sheet extent reduction, by holding orography fixed and focusing on idealised sensitivity experiments, we demonstrate that ice sheets play a critical role in modulating climate feedbacks in response to warming.

This raises potential research questions for future investigation. We believe that Reconstructing and applying Late Pliocene paleogeography remains an important avenue for future experiments and an extended set of sensitivity experiments would provide valuable insights into future climate change and even reduce existing model biases. Experiments would include : Freshwater hosing These include a freshwater hosing experiment introducing a redistributed flux equivalent to the ice sheet volume that is reduced in LP relative to PI; Application of reconstructed LP paleogeography (topography and bathymetry); Increased greenhouse gas forcing; Interactive ice sheets . the Late Pliocene relative to the pre-industrial; the implementation of the reconstructed orography changes intrinsic to the PlioMIP3 guidelines for the ice-sheet sensitivity experiments to assess how orographic changes interact with albedo and freshwater forcing; experiments with various concentrations of imposed atmospheric CO_2 forcing; and the implementation of interactive ice sheets to capture the transient nature of ice-climate feedbacks.

Thus, we conclude that the reduction of AIS primarily influences the circulation of the Antarctic and Southern basins. By isolating the albedo effectclimatic response to ice sheet extent reduction, our study provides a foundational understanding of how ice sheet loss, independent of freshwater input and orographic changes, can significantly alter Southern Hemisphere climate dynamics. We have demonstrated even under present trends, the ability of the Southern Ocean to ventilate the deep ocean is at significant risk. These insights are critical for refining future climate modelsand identifying early signals of ice sheet retreat, offering a clearer picture of the potential pathways and risks associated with polar ice sheet instability.

Author contributions. Conceptualization, K.P., F.D.A.O.M., Q.Z.; methodology, K.P., F.D.A.O.M.; formal analysis, K.P., F.D.A.O.M.; investigation, K.P., F.D.A.O.M.; resources, K.P., Q.Z.; data curation, K.P.; writing–original draft preparation, K.P.; writing–review and editing, K.P., F.D.A.O.M., Q.Z.; visualization, K.P. F.D.A.O.M.; project administration, Q.Z.

Competing interests. The authors declare no conflict of interest.

Acknowledgements. This work was supported by the Swedish Research Council (Vetenskapsrådet, grant no. 2022-03129)

The data analyses were performed using resources provided by the ECMWF's computing and archive facilities and Swedish National Infrastructure for Computing (SNIC) at the National Supercomputer Centre (NSC), which is partially funded by the Swedish Research Council through grant agreement no. 2022-06725.

References

Changing State of the Climate System, in: Climate Change 2021: The Physical Science Basis. Contribution of Working Group I to the Sixth Assessment Report of the Intergovernmental Panel on Climate Change, edited by Gulev, S., Thorne, P., Ahn, J., Dentener, F., Domingues, C., Gerland, S., Gong, D., Kaufman, D., Nnamchi, H., Quaas, J., Sathyendranath, S., Smith, S., Trewin, B., von Schuckmann, K., and Vose, R., Cambridge University Press, Cambridge, https://doi.org/10.1017/9781009157896.004, 2022.

Armstrong McKay, D. I., Staal, A., Abrams, J. F., Winkelmann, R., Sakschewski, B., Loriani, S., Fetzer, I., Cornell, S. E., Rockström, J., and Lenton, T. M.: Exceeding 1.5°C global warming could trigger multiple climate tipping points, Science, 377, eabn7950, https://doi.org/10.1126/science.abn7950, 2022.

Balsamo, G., Beljaars, A., Scipal, K., Viterbo, P., Van Den Hurk, B., Hirschi, M., and Betts, A. K.: A Revised Hydrology for the ECMWF Model: Verification from Field Site to Terrestrial Water Storage and Impact in the Integrated Forecast System, Journal of Hydrometeorology, 10, 623–643, https://doi.org/10.1175/2008JHM1068.1, 2009.

Beadling, R. L., Krasting, J. P., Griffies, S. M., Hurlin, W. J., Bronselaer, B., Russell, J. L., MacGilchrist, G. A., Tesdal, J., and Winton, M.: Importance of the Antarctic Slope Current in the Southern Ocean Response to Ice Sheet Melt and Wind Stress Change, Journal of Geophysical Research: Oceans, 127, e2021JC017 608, https://doi.org/10.1029/2021JC017608, 2022.

Buizert, C., Sigl, M., Severi, M., Markle, B. R., Wettstein, J. J., McConnell, J. R., Pedro, J. B., Sodemann, H., Goto-Azuma, K., Kawamura, K., Fujita, S., Motoyama, H., Hirabayashi, M., Uemura, R., Stenni, B., Parrenin, F., He, F., Fudge, T. J., and Steig, E. J.: Abrupt ice-age shifts in southern westerly winds and Antarctic climate forced from the north, Nature, 563, 681–685, https://doi.org/10.1038/s41586-018-0727-5, 2018.

Burls, N. J., Fedorov, A. V., Sigman, D. M., Jaccard, S. L., Tiedemann, R., and Haug, G. H.: Active Pacific meridional overturning circulation (PMOC) during the warm Pliocene, Science Advances, 3, e1700 156, https://doi.org/10.1126/sciadv.1700156, 2017.

Cai, W., Zheng, X.-T., Weller, E., Collins, M., Cowan, T., Lengaigne, M., Yu, W., and Yamagata, T.: Projected response of the Indian Ocean Dipole to greenhouse warming, Nature Geoscience, 6, 999–1007, https://doi.org/10.1038/ngeo2009, 2013.

Cao, N., Zhang, Q., Power, K. E., Schenk, F., Wyser, K., and Yang, H.: The role of internal feedbacks in sustaining multi-centennial variability of the Atlantic Meridional Overturning Circulation revealed by EC-Earth3-LR simulations, Earth and Planetary Science Letters, 621, 118 372, https://doi.org/10.1016/j.epsl.2023.118372, 2023.

Chandan, D. and Peltier, W. R.: On the mechanisms of warming the mid-Pliocene and the inference of a hierarchy of climate sensitivities with relevance to the understanding of climate futures, Climate of the Past, 14, 825–856, https://doi.org/10.5194/cp-14-825-2018, 2018.

Chen, J., Zhang, Q., Huang, W., Lu, Z., Zhang, Z., and Chen, F.: Northwestward shift of the northern boundary of the East Asian summer monsoon during the mid-Holocene caused by orbital forcing and vegetation feedbacks, Quaternary Science Reviews, 268, 107 136, https://doi.org/10.1016/j.quascirev.2021.107136, 2021.

Chen, J., Zhang, Q., Kjellström, E., Lu, Z., and Chen, F.: The Contribution of Vegetation Climate Feedback and Resultant Sea Ice Loss to Amplified Arctic Warming During the MidHolocene, Geophysical Research Letters, 49, https://doi.org/10.1029/2022GL098816, 2022.

Clark, P. U., Alley, R. B., and Pollard, D.: Northern Hemisphere Ice-Sheet Influences on Global Climate Change, Science, 286, 1104–1111, https://doi.org/10.1126/science.286.5442.1104, 1999.

Craig, A., Valcke, S., and Coquart, L.: Development and performance of a new version of the OASIS coupler, OASIS3-MCT_3.0, Geoscientific Model Development, 10, 3297–3308, https://doi.org/10.5194/gmd-10-3297-2017, 2017.

de Nooijer, W., Zhang, Q., Li, Q., Zhang, Q., Li, X., Zhang, Z., Guo, C., Nisancioglu, K. H., Haywood, A. M., Tindall, J. C., Hunter, S. J., Dowsett, H. J., Stepanek, C., Lohmann, G., Otto-Bliesner, B. L., Feng, R., Sohl, L. E., Chandler, M. A., Tan, N., Contoux, C., Ramstein, G., Baatsen, M. L. J., von der Heydt, A. S., Chandan, D., Peltier, W. R., Abe-Ouchi, A., Chan, W.-L., Kamae, Y., and Brierley, C. M.: Evaluation of Arctic warming in mid-Pliocene climate simulations, Climate of the Past, 16, 2325–2341, https://doi.org/10.5194/cp-16-2325-2020, 2020.

Doddridge, E. W. and Marshall, J.: Modulation of the Seasonal Cycle of Antarctic Sea Ice Extent Related to the Southern Annular Mode, Geophysical Research Letters, 44, 9761–9768, https://doi.org/10.1002/2017GL074319, 2017.

Dolan, A. M., Koenig, S., Hill, D. J., Haywood, A. M., and DeConto, R.: Pliocene Ice Sheet Modelling Intercomparison Project (PLISMIP) – experimental design, Geoscientific Model Development, 5, 963–974, https://doi.org/10.5194/gmd-5-963-2012, 2012.

Dolan, A. M., de Boer, B., Bernales, J., Hill, D. J., and Haywood, A. M.: High climate model dependency of Pliocene Antarctic ice-sheet predictions, Nature Communications, 9, 2799, https://doi.org/10.1038/s41467-018-05179-4, 2018.

Dowsett, H., Barron, J., Poore, R., Thompson, R., Cronin, T., Ishman, S., and Willard, D.: Middle Pliocene paleoenvironmental reconstruction: PRISM2, Tech. rep., USGS, http://pubs.usgs.gov/openfile/of99-535, 1999.

Döscher, R., Acosta, M., Alessandri, A., Anthoni, P., Arsouze, T., Bergman, T., Bernardello, R., Boussetta, S., Caron, L.-P., Carver, G., Castrillo, M., Catalano, F., Cvijanovic, I., Davini, P., Dekker, E., Doblas-Reyes, F. J., Docquier, D., Echevarria, P., Fladrich, U., Fuentes-Franco, R., Gröger, M., v. Hardenberg, J., Hieronymus, J., Karami, M. P., Keskinen, J.-P., Koenigk, T., Makkonen, R., Massonnet, F., Ménégoz, M., Miller, P. A., Moreno-Chamarro, E., Nieradzik, L., van Noije, T., Nolan, P., O'Donnell, D., Ollinaho, P., van den Oord, G., Ortega, P., Prims, O. T., Ramos, A., Reerink, T., Rousset, C., Ruprich-Robert, Y., Le Sager, P., Schmith, T., Schrödner, R., Serva, F., Sicardi, V., Sloth Madsen, M., Smith, B., Tian, T., Tourigny, E., Uotila, P., Vancoppenolle, M., Wang, S., Wårlind, D., Willén, U., Wyser, K., Yang, S., Yepes-Arbós, X., and Zhang, Q.: The EC-Earth3 Earth system model for the Coupled Model Intercomparison Project 6, Geoscientific Model Development, 15, 2973–3020, https://doi.org/10.5194/gmd-15-2973-2022, 2022.

Eyring, V., Bony, S., Meehl, G. A., Senior, C. A., Stevens, B., Stouffer, R. J., and Taylor, K. E.: Overview of the Coupled Model Intercomparison Project Phase 6 (CMIP6) experimental design and organization, Geoscientific Model Development, 9, 1937–1958, https://doi.org/10.5194/gmd-9-1937-2016, 2016.

Feng, R., Otto-Bliesner, B. L., Fletcher, T. L., Tabor, C. R., Ballantyne, A. P., and Brady, E. C.: Amplified Late Pliocene terrestrial warmth in northern high latitudes from greater radiative forcing and closed Arctic Ocean gateways, Earth and Planetary Science Letters, 466, 129–138, https://doi.org/10.1016/j.epsl.2017.03.006, 2017.

Gerber, E. P. and Vallis, G. K.: Eddy–Zonal Flow Interactions and the Persistence of the Zonal Index, Journal of the Atmospheric Sciences, 64, 3296–3311, https://doi.org/10.1175/JAS4006.1, 2007.

Gorte, T., Lovenduski, N. S., Nissen, C., and Lenaerts, J. T. M.: Antarctic Ice Sheet Freshwater Discharge Drives Substantial Southern Ocean Changes Over the 21st Century, Geophysical Research Letters, 50, e2023GL104 949, https://doi.org/10.1029/2023GL104949, 2023.

Greene, C. A., Gardner, A. S., Wood, M., and Cuzzone, J. K.: Ubiquitous acceleration in Greenland Ice Sheet calving from 1985 to 2022, Nature, 625, 523–528, https://doi.org/10.1038/s41586-023-06863-2, 2024.

Han, Z., Power, K., Li, G., and Zhang, Q.: Impacts of Mid-Pliocene Ice Sheets and Vegetation on Afro-Asian Summer Monsoon Rainfall Revealed by EC-Earth Simulations, Geophysical Research Letters, 51, e2023GL106 145, https://doi.org/10.1029/2023GL106145, 2024.

Haywood, Dowsett, H. J., Otto-Bliesner, B., Chandler, M. A., Dolan, A. M., Hill, D. J., Lunt, D. J., Robinson, M. M., Rosenbloom, N., Salzmann, U., and Sohl, L. E.: Pliocene Model Intercomparison Project (PlioMIP): experimental design and boundary conditions (Experiment 1), Geoscientific Model Development, 3, 227–242, https://doi.org/10.5194/gmd-3-227-2010, 2010.

Haywood, Dowsett, H. J., Dolan, A. M., Rowley, D., Abe-Ouchi, A., Otto-Bliesner, B., Chandler, M. A., Hunter, S. J., Lunt, D. J., Pound, M., and Salzmann, U.: The Pliocene Model Intercomparison Project (PlioMIP) Phase 2: scientific objectives and experimental design, Climate of the Past, 12, 663–675, https://doi.org/10.5194/cp-12-663-2016, 2016a.

Haywood, Tindall, J. C., Dowsett, H. J., Dolan, A. M., Foley, K. M., Hunter, S. J., Hill, D. J., Chan, W.-L., Abe-Ouchi, A., Stepanek, C., Lohmann, G., Chandan, D., Peltier, W. R., Tan, N., Contoux, C., Ramstein, G., Li, X., Zhang, Z., Guo, C., Nisancioglu, K. H., Zhang, Q., Li, Q., Kamae, Y., Chandler, M. A., Sohl, L. E., Otto-Bliesner, B. L., Feng, R., Brady, E. C., von der Heydt, A. S., Baatsen, M. L. J., and Lunt, D. J.: The Pliocene Model Intercomparison Project Phase 2: large-scale climate features and climate sensitivity, Climate of the Past, 16, 2095–2123, https://doi.org/10.5194/cp-16-2095-2020, 2020.

Haywood, A., Burton, L., Dolan, A., Dowsett, H., Fletcher, T., Hill, D., Hunter, S., and Tindall, J.: PlioMIP3 A Science Programme Proposal to the Community, other, display, https://doi.org/10.5194/egusphere-gc10-pliocene-61, 2022.

Haywood, A. M., Hill, D. J., Dolan, A. M., Otto-Bliesner, B. L., Bragg, F., Chan, W.-L., Chandler, M. A., Contoux, C., Dowsett, H. J., Jost, A., Kamae, Y., Lohmann, G., Lunt, D., Abe-Ouchi, A., Pickering, S. J., Ramstein, G., Rosenbloom, N., Salzmann, U., Sohl, L., Stepanek, C., Ueda, H., Yan, Q., and Zhang, Z.: Large-scale features of Pliocene climate: results from the Pliocene Model Intercomparison Project, Climate of the Past, 9, 191–209, https://doi.org/10.5194/cp-9-191-2013, 2013.

Haywood, A. M., Dowsett, H. J., and Dolan, A. M.: Integrating geological archives and climate models for the mid-Pliocene warm period, Nature Communications, 7, 10 646, https://doi.org/10.1038/ncomms10646, 2016b.

Haywood, A. M., Tindall, J. C., Burton, L. E., Chandler, M. A., Dolan, A. M., Dowsett, H. J., Feng, R., Fletcher, T. L., Foley, K. M., Hill, D. J., Hunter, S. J., Otto-Bliesner, B. L., Lunt, D. J., Robinson, M. M., and Salzmann, U.: Pliocene Model Intercomparison Project Phase 3 (PlioMIP3) – Science plan and experimental design, Global and Planetary Change, 232, 104 316, https://doi.org/10.1016/j.gloplacha.2023.104316, 2024.

Herold, N., Huber, M., Müller, R. D., and Seton, M.: Modeling the Miocene climatic optimum: Ocean circulation, Paleoceanography, 27, 2010PA002 041, https://doi.org/10.1029/2010PA002041, 2012.

Hill, D.: Modelling Earth's cryosphere during Peak Pliocene Warmth, Ph.D. thesis, University of Bristol /British Antarctic Survey, 2009.

Hill, D., Haywood, A., Hindmarsh, R., and Valdes, P.: Characterizing ice sheets during the Pliocene: evidence from data and models, in: Deep-Time Perspectives on Climate Change: Marrying the Signal from Computer Models and Biological Proxies, edited by Williams, M., Haywood, A., Gregory, F., and Schmidt, D., pp. 517–538, The Geological Society of London on behalf of The Micropalaeontological Society, first edn., https://doi.org/10.1144/TMS002.24, 2007.

Hutchinson, D. K., Menviel, L., Meissner, K. J., and Hogg, A. M.: East Antarctic warming forced by ice loss during the Last Interglacial, Nature Communications, 15, 1026, https://doi.org/10.1038/s41467-024-45501-x, 2024.

Kidston, J., Vallis, G. K., Dean, S. M., and Renwick, J. A.: Can the Increase in the Eddy Length Scale under Global Warming Cause the Poleward Shift of the Jet Streams?, Journal of Climate, 24, 3764–3780, https://doi.org/10.1175/2010JCLI3738.1, 2011.

Kim, S. and Crowley, T. J.: Increased Pliocene North Atlantic Deep Water: Cause or consequence of Pliocene warming?, Paleoceanography, 15, 451–455, https://doi.org/10.1029/1999PA000459, 2000.

Koenigk, T., Brodeau, L., Graversen, R. G., Karlsson, J., Svensson, G., Tjernström, M., Willén, U., and Wyser, K.: Arctic climate change in 21st century CMIP5 simulations with EC-Earth, Climate Dynamics, 40, 2719–2743, https://doi.org/10.1007/s00382-012-1505-y, 2013.

Kusahara, K., Williams, G. D., Tamura, T., Massom, R., and Hasumi, H.: Dense shelf water spreading from A ntarctic coastal polynyas to the deep S outhern <span style="font-

variant:small-caps;">O cean: A regional circumpolar model study, Journal of Geophysical Research: Oceans, 122, 6238–6253, https://doi.org/10.1002/2017JC012911, 2017.

Lord, N. S., Crucifix, M., Lunt, D. J., Thorne, M. C., Bounceur, N., Dowsett, H., O'Brien, C. L., and Ridgwell, A.: Emulation of long-term changes in global climate: application to the late Pliocene and future, Climate of the Past, 13, 1539–1571, https://doi.org/10.5194/cp-13-1539-2017, 2017.

Lunt, D. J., Haywood, A. M., Schmidt, G. A., Salzmann, U., Valdes, P. J., Dowsett, H. J., and Loptson, C. A.: On the causes of mid-Pliocene warmth and polar amplification, Earth and Planetary Science Letters, 321-322, 128–138, https://doi.org/10.1016/j.epsl.2011.12.042, 2012.

Madec, M.: NEMO Ocean Engine. Note du Pole de modélisation, Tech. rep., Institut Pierre-Simon Laplace (IPSL), Paris, France, 2008.

Marshall, G. J.: Trends in the Southern Annular Mode from Observations and Reanalyses, Journal of Climate, 16, 4134–4143, https://doi.org/10.1175/1520-0442(2003)016<4134:TITSAM>2.0.CO;2, 2003.

Menviel, L., Timmermann, A., Timm, O. E., and Mouchet, A.: Climate and biogeochemical response to a rapid melting of the West Antarctic Ice Sheet during interglacials and implications for future climate: CLIMATE RESPONSE TO ANTARCTIC MELTWATER, Paleoceanography, 25, n/a–n/a, https://doi.org/10.1029/2009PA001892, 2010.

Menviel, L. C., Spence, P., Kiss, A. E., Chamberlain, M. A., Hayashida, H., England, M. H., and Waugh, D.: Enhanced Southern Ocean CO_2 outgassing as a result of stronger and poleward shifted southern hemispheric westerlies, Biogeosciences, 20, 4413–4431, https://doi.org/10.5194/bg-20-4413-2023, 2023.

Morioka, Y., Manabe, S., Zhang, L., Delworth, T. L., Cooke, W., Nonaka, M., and Behera, S. K.: Antarctic sea ice multidecadal variability triggered by Southern Annular Mode and deep convection, Communications Earth & Environment, 5, 633, https://doi.org/10.1038/s43247-024-01783-z, 2024.

Naish, T., Powell, R., Levy, R., Wilson, G., Scherer, R., Talarico, F., Krissek, L., Niessen, F., Pompilio, M., Wilson, T., Carter, L., DeConto, R., Huybers, P., McKay, R., Pollard, D., Ross, J., Winter, D., Barrett, P., Browne, G., Cody, R., Cowan, E., Crampton, J., Dunbar, G., Dunbar, N., Florindo, F., Gebhardt, C., Graham, I., Hannah, M., Hansaraj, D., Harwood, D., Helling, D., Henrys, S., Hinnov, L., Kuhn, G., Kyle, P., Läufer, A., Maffioli, P., Magens, D., Mandernack, K., McIntosh, W., Millan, C., Morin, R., Ohneiser, C., Paulsen, T., Persico, D., Raine, I., Reed, J., Riesselman, C., Sagnotti, L., Schmitt, D., Sjunneskog, C., Strong, P., Taviani, M., Vogel, S., Wilch, T., and Williams, T.: Obliquity-paced Pliocene West Antarctic ice sheet oscillations, Nature, 458, 322–328, https://doi.org/10.1038/nature07867, 2009.

Naughten, K. A., Holland, P. R., and De Rydt, J.: Unavoidable future increase in West Antarctic ice-shelf melting over the twenty-first century, Nature Climate Change, 13, 1222–1228, https://doi.org/10.1038/s41558-023-01818-x, 2023.

Noble, T. L., Rohling, E. J., Aitken, A. R. A., Bostock, H. C., Chase, Z., Gomez, N., Jong, L. M., King, M. A., Mackintosh, A. N., McCormack, F. S., McKay, R. M., Menviel, L., Phipps, S. J., Weber, M. E., Fogwill, C. J., Gayen, B., Golledge, N. R., Gwyther, D. E., Hogg, A. M., Martos, Y. M., Pena-Molino, B., Roberts, J., Van De Flierdt, T., and Williams, T.: The Sensitivity of the Antarctic Ice Sheet to a Changing Climate: Past, Present, and Future, Reviews of Geophysics, 58, e2019RG000 663, https://doi.org/10.1029/2019RG000663, 2020.

Orsi, A., Johnson, G., and Bullister, J.: Circulation, mixing, and production of Antarctic Bottom Water, Progress in Oceanography, 43, 55–109, https://doi.org/10.1016/S0079-6611(99)00004-X, 1999.

Otto-Bliesner, B. L., Braconnot, P., Harrison, S. P., Lunt, D. J., Abe-Ouchi, A., Albani, S., Bartlein, P. J., Capron, E., Carlson, A. E., Dutton, A., Fischer, H., Goelzer, H., Govin, A., Haywood, A., Joos, F., LeGrande, A. N., Lipscomb, W. H., Lohmann, G., Mahowald, N., Nehrbass-Ahles, C., Pausata, F. S. R., Peterschmitt, J.-Y., Phipps, S. J., Renssen, H., and Zhang, Q.: The PMIP4 contribution to CMIP6 –

Part 2: Two interglacials, scientific objective and experimental design for Holocene and Last Interglacial simulations, Geoscientific Model Development, 10, 3979–4003, https://doi.org/10.5194/gmd-10-3979-2017, 2017.

Pardo, P. C., Pérez, F. F., Velo, A., and Gilcoto, M.: Water masses distribution in the Southern Ocean: Improvement of an extended OMP (eOMP) analysis, Progress in Oceanography, 103, 92–105, https://doi.org/10.1016/j.pocean.2012.06.002, 2012.

Pollard, D., DeConto, R. M., and Alley, R. B.: Potential Antarctic Ice Sheet retreat driven by hydrofracturing and ice cliff failure, Earth and Planetary Science Letters, 412, 112–121, https://doi.org/10.1016/j.epsl.2014.12.035, 2015.

Power, K. and Zhang, Q.: The impacts of reduced ice sheets, vegetation, and elevated CO2 on future Arctic climates, Arctic, Antarctic, and Alpine Research, 56, 2433 860, https://doi.org/10.1080/15230430.2024.2433860, 2024.

Power, K., Lu, Z., and Zhang, Q.: Impacts of large-scale Saharan solar farms on the global terrestrial carbon cycle, Environmental Research Letters, 18, 104 009, https://doi.org/10.1088/1748-9326/acf7d8, 2023.

Pörtner, H.-O., Roberts, D. C., Tignor, M. M. B., Poloczanska, E. S., Mintenbeck, K., Alegría, A., Craig, M., Langsdorf, S., Löschke, S., Möller, V., Okem, A., and Rama, B., eds.: Climate Change 2022: Impacts, Adaptation and Vulnerability. Contribution of Working Group II to the Sixth Assessment Report of the Intergovernmental Panel on Climate Change., Cambridge University Press, 2022.

Ramadhan, A., Marshall, J., Meneghello, G., Illari, L., and Speer, K.: Observations of Upwelling and Downwelling Around Antarctica Mediated by Sea Ice, Frontiers in Marine Science, 9, 864 808, https://doi.org/10.3389/fmars.2022.864808, 2022.

Roach, L. A., Mankoff, K. D., Romanou, A., Blanchard-Wrigglesworth, E., Haine, T. W. N., and Schmidt, G. A.: Winds and Meltwater Together Lead to Southern Ocean Surface Cooling and Sea Ice Expansion, Geophysical Research Letters, 50, e2023GL105 948, https://doi.org/10.1029/2023GL105948, 2023.

Schmidt, C., Morrison, A. K., and England, M. H.: Wind– and Sea-Ice–Driven Interannual Variability of Antarctic Bottom Water Formation, Journal of Geophysical Research: Oceans, 128, e2023JC019 774, https://doi.org/10.1029/2023JC019774, 2023.

Screen, J. A., Simmonds, I., and Keay, K.: Dramatic interannual changes of perennial Arctic sea ice linked to abnormal summer storm activity, Journal of Geophysical Research, 116, D15 105, https://doi.org/10.1029/2011JD015847, 2011.

Sidorenko, D., Danilov, S., Streffing, J., Fofonova, V., Goessling, H. F., Scholz, P., Wang, Q., Androsov, A., Cabos, W., Juricke, S., Koldunov, N., Rackow, T., Sein, D. V., and Jung, T.: AMOC Variability and Watermass Transformations in the AWI Climate Model, Journal of Advances in Modeling Earth Systems, 13, e2021MS002 582, https://doi.org/10.1029/2021MS002582, 2021.

Silvano, A., Purkey, S., Gordon, A. L., Castagno, P., Stewart, A. L., Rintoul, S. R., Foppert, A., Gunn, K. L., Herraiz-Borreguero, L., Aoki, S., Nakayama, Y., Naveira Garabato, A. C., Spingys, C., Akhoudas, C. H., Sallée, J.-B., De Lavergne, C., Abrahamsen, E. P., Meijers, A. J. S., Meredith, M. P., Zhou, S., Tamura, T., Yamazaki, K., Ohshima, K. I., Falco, P., Budillon, G., Hattermann, T., Janout, M. A., Llanillo, P., Bowen, M. M., Darelius, E., Østerhus, S., Nicholls, K. W., Stevens, C., Fernandez, D., Cimoli, L., Jacobs, S. S., Morrison, A. K., Hogg, A. M., Haumann, F. A., Mashayek, A., Wang, Z., Kerr, R., Williams, G. D., and Lee, W. S.: Observing Antarctic Bottom Water in the Southern Ocean, Frontiers in Marine Science, 10, 1221 701, https://doi.org/10.3389/fmars.2023.1221701, 2023.

Singh, H. K. A., Bitz, C. M., and Frierson, D. M. W.: The Global Climate Response to Lowering Surface Orography of Antarctica and the Importance of Atmosphere–Ocean Coupling, Journal of Climate, 29, 4137–4153, https://doi.org/10.1175/JCLI-D-15-0442.1, 2016.

Song, P., Scholz, P., Knorr, G., Sidorenko, D., Timmermann, R., and Lohmann, G.: Regional conditions determine thresholds of accelerated Antarctic basal melt in climate projection, Nature Climate Change, https://doi.org/10.1038/s41558-025-02306-0, 2025.

Steig, E. J., Huybers, K., Singh, H. A., Steiger, N. J., Ding, Q., Frierson, D. M. W., Popp, T., and White, J. W. C.: Influence of West Antarctic Ice Sheet collapse on Antarctic surface climate, Geophysical Research Letters, 42, 4862–4868, https://doi.org/10.1002/2015GL063861, 2015.

Stocker, T. F., Qin, D., Plattner, G.-K., Tignor, M., Allen, S., Boschung, J., Nauels, A., Xia, Y., Bex, V., and Midgley, P.: IPCC, 2013: Climate Change 2013: The Physical Science Basis. Contribution of Working Group I to the Fifth Assessment Report of the Intergovernmental Panel on Climate Change., Cambridge University Press, Cambridge, 2013.

Talley, L.: Distribution and Formation of North Pacific Intermediate Water, Journal of Physical Oceanography, 23, 517–537, 1993.

Talley, L., Feely, R., Sloyan, B., Wanninkhof, R., Baringer, M., Bullister, J., Carlson, C., Doney, S., Fine, R., Firing, E., Gruber, N., Hansell, D., Ishii, M., Johnson, G., Katsumata, K., Key, R., Kramp, M., Langdon, C., Macdonald, A., Mathis, J., McDonagh, E., Mecking, S., Millero, F., Mordy, C., Nakano, T., Sabine, C., Smethie, W., Swift, J., Tanhua, T., Thurnherr, A., Warner, M., and Zhang, J.-Z.: Changes in Ocean Heat, Carbon Content, and Ventilation: A Review of the First Decade of GO-SHIP Global Repeat Hydrography, Annual Review of Marine Science, 8, 185–215, https://doi.org/10.1146/annurev-marine-052915-100829, 2016.

Tamsitt, V., Drake, H. F., Morrison, A. K., Talley, L. D., Dufour, C. O., Gray, A. R., Griffies, S. M., Mazloff, M. R., Sarmiento, J. L., Wang, J., and Weijer, W.: Spiraling pathways of global deep waters to the surface of the Southern Ocean, Nature Communications, 8, 172, https://doi.org/10.1038/s41467-017-00197-0, 2017.

Thompson, D. W. J. and Wallace, J. M.: Annular Modes in the Extratropical Circulation. Part I: Month-to-Month Variability*, Journal of Climate, 13, 1000–1016, https://doi.org/10.1175/1520-0442(2000)013<1000:AMITEC>2.0.CO;2, 2000.

Thompson, D. W. J., Baldwin, M. P., and Solomon, S.: Stratosphere–Troposphere Coupling in the Southern Hemisphere, Journal of the Atmospheric Sciences, 62, 708–715, https://doi.org/10.1175/JAS-3321.1, 2005.

Thompson, D. W. J., Solomon, S., Kushner, P. J., England, M. H., Grise, K. M., and Karoly, D. J.: Signatures of the Antarctic ozone hole in Southern Hemisphere surface climate change, Nature Geoscience, 4, 741–749, https://doi.org/10.1038/ngeo1296, 2011.

Trevena, J., Sijp, W. P., and England, M. H.: Stability of Antarctic Bottom Water Formation to Freshwater Fluxes and Implications for Global Climate, Journal of Climate, 21, 3310–3326, https://doi.org/10.1175/2007JCLI2212.1, 2008.

Vancoppenolle, M., Bouillon, S., Fichefet, T., Goosse, H., Lecomte, O., Morales Maqueda, M., and Made, M.: The Louvain-la-Neuve sea ice model, Notes du pole de modélisation, Tech. rep., Institut Pierre-Simon Laplace (IPSL), Paris, France, 2012.

Watson, A. J., Vallis, G. K., and Nikurashin, M.: Southern Ocean buoyancy forcing of ocean ventilation and glacial atmospheric CO2, Nature Geoscience, 8, 861–864, https://doi.org/10.1038/ngeo2538, 2015.

Weiffenbach, J. E., Dijkstra, H. A., Von Der Heydt, A. S., Abe-Ouchi, A., Chan, W.-L., Chandan, D., Feng, R., Haywood, A. M., Hunter, S. J., Li, X., Otto-Bliesner, B. L., Peltier, W. R., Stepanek, C., Tan, N., Tindall, J. C., and Zhang, Z.: Highly stratified mid-Pliocene Southern Ocean in PlioMIP2, Climate of the Past, 20, 1067–1086, https://doi.org/10.5194/cp-20-1067-2024, 2024.

Xie, A., Zhu, J., Kang, S., Qin, X., Xu, B., and Wang, Y.: Polar amplification comparison among Earth's three poles under different socioeconomic scenarios from CMIP6 surface air temperature, Scientific Reports, 12, 16 548, https://doi.org/10.1038/s41598-022-21060-3, 2022.

Yeung, N. K.-H., Menviel, L., Meissner, K. J., Choudhury, D., Ziehn, T., and Chamberlain, M. A.: Last Interglacial subsurface warming on the Antarctic shelf triggered by reduced deep-ocean convection, Communications Earth & Environment, 5, 212, https://doi.org/10.1038/s43247-024-01383-x, 2024.

Zhang, L., Delworth, T. L., Cooke, W., and Yang, X.: Natural variability of Southern Ocean convection as a driver of observed climate trends, Nature Climate Change, 9, 59–65, https://doi.org/10.1038/s41558-018-0350-3, 2019.

Zhang, Q., Berntell, E., Axelsson, J., Chen, J., Han, Z., de Nooijer, W., Lu, Z., Li, Q., Zhang, Q., Wyser, K., and Yang, S.: Simulating the mid-Holocene, last interglacial and mid-Pliocene climate with EC-Earth3-LR, Geoscientific Model Development, 14, 1147–1169, https://doi.org/10.5194/gmd-14-1147-2021, 2021.